Analysis and optimisation of H_2 production from crude glycerol by steam reforming using a novel two step process

J. Remón, C. Jarauta-Córdoba, L. García*, J. Arauzo

Thermochemical Processes Group (GPT), Aragón Institute for Engineering Research (I3A), Universidad de Zaragoza. Mariano Esquillor s/n, E-50018 Zaragoza, Spain.
*Corresponding author. Tel: +34 976 762194; Fax.: +34 976 761879; e-mail: luciag@unizar.es

ABSTRACT

This work studies the valorisation of biodiesel-derived glycerol to produce a hydrogen rich gas by means of a two-step sequential process. Firstly, the crude glycerol was purified with acetic acid to reduce problematical impurities. The effect of the final pH (5-7) on the neutralisation process was addressed and it was found that a pH of 6 provided the best phase separation and the greatest glycerol purity. Secondly, the refined glycerol was upgraded by catalytic steam reforming and this step was theoretically and experimentally studied. The theoretical study analyses the effect of the temperature (400-700 ºC), glycerol concentration (10-50 wt.%) and N_2 (225-1347 cm^3 STP/min) and liquid flow (0.5-1 mL/min) rates on the thermodynamic composition of the gas. The results show that the temperature and glycerol concentration exerted the greatest influence on the thermodynamics. The experimental study considers the effect of the temperature (400-700 ºC), glycerol concentration (10-50 wt.%) and spatial time (3-17 g catalyst min/ g glycerol) on the product distribution in carbon basis (gas, liquid and solid) and on the composition of the gas and liquid phases. The experiments were planned according to a 2 level 3 factor Box-Wilson Central Composite Face Centred (CCF, α: ± 1) design, which is suitable for studying the influence of each variable as well as all the possible interactions between variables. The results were analysed with an analysis of variance (ANOVA) with 95% confidence, enabling the optimisation of

the process. The gas phase was made up of a mixture of H_2 (65-95 vol.%), CO_2 (2-29 vol.%), CO (0-18 vol.%) and CH_4 (0-5 vol.%). Temperatures of 550 ºC and above enabled thermodynamic compositions for the gas to be achieved and helped diminish carbon formation. A possible optimum for H_2 production was found at a temperature of around 680 ºC, feeding a glycerol solution of 37 wt.% and using a spatial time of 3 g catalyst min/g glycerol. These conditions provide a 95% carbon conversion to gas, having the following composition: 67 vol.% H_2, 22 vol.% CO_2, 11 vol.% CO and 1 vol.% CH_4.

Keywords: crude glycerol, glycerol purification, hydrogen production, catalytic steam reforming

1. Introduction

Widespread environmental concerns and stricter regulations for fuels have led to a considerable increase in worldwide biodiesel production. This biofuel represents a promising alternative energy source that helps to reduce net CO_2 emissions. Its production is commonly based on the transesterification of triglycerides using an alcohol (methanol or ethanol) in the presence of a catalyst (commonly basic and homogeneous, such as NaOH or KOH). However, despite the environmental benefits of biodiesel, its production originates glycerol as a by-product (10 kg of biodiesel yields approximately 1 kg of crude glycerol). This scenario could create a surplus of crude glycerol that might not be absorbed by its current market [1]. Therefore new alternatives should be considered and investigated for the treatment of this by-product bearing in mind that its valorisation could be beneficial for the improvement of the biodiesel economy and sustainability [2].

There are two main options to deal with this biodiesel-derived glycerol. The first consists of its purification to obtain high purity glycerol for use in, for example, the food, cosmetics and pharmaceutical industries [1, 3]. The second option is to upgrade crude glycerol to produce different value-added chemicals and/or energy using different valorisation routes such as gasification, steam reforming, aqueous phase reforming and supercritical reforming, among others [4, 5].

This work is focused on H_2 production from crude glycerol, a biodiesel by-product, which consists not only of glycerol but also of many other chemicals [1]. As these impurities can significantly reduce the yields and efficiencies of the valorisation

processes, an intermediate option has been addressed in this work. This consists of a first purification of the crude glycerol up to an appropriate level to reduce troublesome impurities without compromising the economy of the whole process, followed by the catalytic steam reforming of the refined glycerol solution produced. In this context, a cost-effective glycerol purification method to produce a purified glycerol solution (85-90% purity) consists of the physical separation of the fatty acid methyl esters (FAMES) and the elimination of the soaps present in the solution by acidification step, together with a subsequent liquid-liquid extraction if necessary. The work of Manosak et al. [1] provides an in depth study of this purification method.

Catalytic steam reforming is a very promising way to produce H_2 and/or syngas from biodiesel-derived glycerol [6]. H_2 can be used in fuel cells to generate energy in biodiesel production plants, while syngas can be used for the production of different chemicals such as methanol, other alcohols and aldehydes in a third generation bio-refinery [7]. Pure H_2 can be obtained from syngas by removing the CO_2 from the syngas. Very interestingly, Dou et al. [8, 9] and Wess et al. [10] studied the production of H_2 from glycerol using a sorption-enhanced process with CO_2 removal. Different Ni-based catalysts were used for this process. In addition, Dou et al. [11] also integrated the reduction of the catalyst into the same process by enhanced-sorption chemical looping of glycerol [12] .

As regards catalytic steam reforming, there are several works focused on studying catalytic activity and the effect of operating conditions on the reforming of glycerol, both theoretically and experimentally [2]. However, the works studying the catalytic steam reforming of crude glycerol [6, 13-17] are scarce. The crude glycerol used in

these works, apart from glycerol, was made up of methanol, inorganic salts, polyglycerols and fatty acid impurities. In some cases, the results obtained with reagent grade and crude glycerol were compared [6, 16]. This comparison revealed that higher coke contents were obtained when crude glycerol was used and indicated that the presence of fatty acid methyl esters in crude glycerol was one of the reasons. However, these global comparisons present contradictory results in some cases.

Slinn et al. [6] found that the conversions and yields with crude glycerol were 70% of those obtained with pure glycerol. They reported that the long chain fatty acid impurities were harder to reform and more likely to form carbon. Dou et al. [15] reported that crude glycerol conversions were slightly higher than those of pure glycerol under the same reaction conditions. It was suggested that the presence of thermally resistant residues was responsible for these differences. The H_2 content using crude glycerol was slightly higher than using pure glycerol. The presence of methanol and FAMES increased the H_2 content compared to that of pure glycerol due to the stoichiometry. In the work of Valliyappan et al. [18] the production of hydrogen and the yield to gas from crude glycerol were higher than those from pure glycerol, while the formation of char was higher for crude glycerol. The authors stated that the presence of KOH in the glycerol solution could favour the gasification reactions and char formation.

Considering this background, this paper reports H_2 production from crude glycerol by a novel two-step process. Acetic acid was used for the purification step, as it has been proved appropriate for glycerol purification without poisoning the catalysts that are habitually used in steam reforming [1]. Firstly, the influence of the pH (5-7) used during the purification of the glycerol phase was analysed and optimised. Secondly, the

catalytic steam reforming of the refined glycerol was studied theoretically and experimentally in a fluidised bed reactor. This glycerol solution still contains some of the acid used in the neutralization, part of the catalyst used in the biodiesel production (KOH), as well as the alcohol (methanol) used during the transesterification reaction. This fluidised bed reactor helps to decrease catalyst deactivation by coking [19] and mitigates its plugging by the accumulation of KOH in the upper part of the bed, as can occur when fixed bed configurations are used for crude glycerol reforming. This accumulation of salts in the catalyst bed was reported in the work of Fermoso et al. [16]. In addition, fluidised bed reactors allow greater production and a better external mass/heat transport between the gas and the solid particles to be achieved in comparison with fixed beds.

The fact that this two step strategy has never been used before for the valorisation of crude glycerol together with the results provided by the in-depth study of the process, where the influence of the operating variables on the product distribution and on the compositions of both the gas and liquid phases has been thoroughly discussed, demonstrate that this work contributes to gaining a better insight into the field of hydrogen production from the glycerol obtained as a by-product in the biodiesel industry.

2. Materials and methods

2.1 Crude glycerol and purification process

The crude glycerol used for this work comes from the transesterification of sunflower oil with methanol, employing potassium hydroxide as a catalyst. The properties of the

crude glycerol determined by means of Total Organic Carbon (TOC), density, viscosity, pH and chemical composition are summarised in Table 1. The chemical composition was calculated by means of a Gas Chromatography-Mass Spectrometry analysis, Karl Fischer titration and ash content. The GC-MS analysis of the glycerol also revealed the presence of a small proportion of some fatty acid methyl esters (FAMES): linoleic ($C_{19}H_{34}O_2$), palmitic ($C_{17}H_{34}O_2$), oleic ($C_{19}H_{36}O_2$), and stearic ($C_{19}H_{38}O_2$). The properties of this crude glycerol are in agreement with those identified in other works reported in the literature [15, 16, 18].

The purification step comprises an initial neutralisation followed by a vacuum distillation to produce the refined glycerol. Acetic acid was employed for the neutralisation and the effect of the pH on the properties of the glycerol phase was analysed. The neutralisation took place at 25 ºC and atmospheric pressure. Acetic acid was added slowly, drop by drop, to 25 mL of crude glycerol. The crude glycerol solution was magnetically stirred at 250 rpm. A pH meter was used to monitor the pH of the solution. Once the final pH was reached, two phases appeared. The rest of the biodiesel and the free fatty acids constituted the upper phase. The bottom phase consisted of a rich-glycerol phase. These two phases were then separated through decantation in a 500 mL separation funnel for 24 h. Final pHs of 5, 6 and 7 were used for the neutralisation step. The initial phase separation velocity was measured and the refined glycerol was characterised. The subsequent vacuum distillation aims to reduce the amount of methanol and acetic acid in the solution, increasing the purity of the glycerol phase. These solutions (after both neutralisation and distillation) were characterised employing the same techniques as for the crude glycerol.

2.2 Theoretical reforming study

The theoretical study analyses the influence on the thermodynamic gas composition (vol.%) of the reforming temperature (400-700 ºC), glycerol concentration (10-50 wt.%), flow rate of N_2 (225-1347 cm^3STP/min) and the liquid flow rate (0.5-1 mL/min).

The feed employed for the simulations include glycerol and the corresponding amounts of CH_3COOH, CH_3OH resulting from the dilution in water of the refined glycerol. For this study different simulations based on a 2 level 4 factor Box-Wilson Central Composite Face Centred (CCF, α: $\pm$ 1) design were carried out. The gas composition (vol.%) was calculated using the Gibbs energy minimisation method. Three different thermodynamic packages (PRSV, Twu-Sim-Tasonee and Lee-Kesler-Plöcker) were used. H_2, CO, CO_2 and CH_4 on the one hand and glycerol, acetic acid, and methanol on the other were selected as possible steam reforming products and non-consumed reagents, respectively, for the Gibbs energy minimisation calculations [4, 20-24]. In addition, the thermodynamic formation of solid C was considered negligible under the operating conditions employed, which is in accordance with the results of other thermodynamic studies [5, 24-27]. The results were analysed by means of an ANOVA test with 95% confidence and the relative influence of the operating variables was calculated using the cause-effect Pareto principle.

2.3 Experimental reforming study

The influence of the reforming temperature (400-700 ºC), glycerol concentration (10-50 wt.%) and ratio mass of the catalyst/glycerol mass flow rate ($W/m_{glycerol}$ = 3-17 g catalyst min/g glycerol) on the catalytic steam reforming process was experimentally studied using a coprecipitated Ni-Co/Al-Mg catalyst in a fluidised bed reactor for 2 h.

The detailed preparation procedure of the catalyst and its characterisation results can be found in our previous communications [19, 28, 29]. This catalyst includes Ni as the active phase. Ni based catalysts meet the challenge of being active and selective towards H_2, although they are susceptible to deactivation by coking. Therefore, the catalyst was modified with Mg and Co. Mg was added as a support modifier enhancing the water adsorption in order to gasify the coke or its precursors, as well as to provide sufficient strength if the process is to take place in a fluidized bed reactor [30, 31]. Co was added as a active phase modifier to enhance the steam reforming and WGS reactions and prevent catalyst deactivation by coking, as a Ni-Co interaction can be formed in the catalyst which reduces the crystallite size [19].

The experimental rig consists of a bench-scale fluidised bed reactor made of stainless steel, with a 2.54 cm inner diameter, operated at atmospheric pressure. The reactor was heated up by means of an electric furnace. The reaction temperature was monitored in situ with a type K thermocouple placed in the bed, and controlled by means of a PDI controller. The catalytic bed consisted of a mixture of catalyst and sand, both with a particle size of 160-320 μm. The refined glycerol solution used for this work, resulting from the dilution in water of the refined glycerol described above, was fed into the reactor by being sprayed through a quartz coaxial injection nozzle placed inside a cooling jacket to avoid the polymerization of non-volatile compounds in the injection system when introducing the feed. The gases emerging from the upper part of the reactor passed through a condensation ice trap. The non-condensable gases continued and passed through a cotton filter. Finally, the gaseous mixture leaving the filter passed to an Agilent P200 micro gas chromatograph equipped with thermal conductivity detectors.

N_2 was used as an internal standard for the quantification of the gas as well as the fluidising agent. A u/u_{mf} ratio of 6 (previously optimised for this reactor) defined as the ratio between the superficial gas velocity and the velocity of the theoretically calculated minimum fluidisation [32] was employed in all the experiments. The fluidisation of the bed was achieved with N_2 and the excess of water of the feed. Therefore, the mass flow rate of N_2 was adjusted depending on the concentration of glycerol and the temperature of the experiment. An appropriate fluidisation regime is very important for the correct development and scale up of the process, as thoroughly discussed in the work of Dou et al. [33]. They reported that the glycerol conversion and H_2 production decreased with increasing the inlet gas velocity (increasing the u/u_{mf} ratio). A detailed description of the installation can be found in our previous communication [19]. However, the rig was slightly modified for this work. A stainless steel fluidised reactor was used instead of the original quartz reactor due to the presence of KOH in the glycerol solution. Additionally, three condensers were used to collect the liquid condensates at intervals of 40 minutes in order to study the evolution over time of the liquid phase.

The experiments were planned according to a 2 level 3 factor Box-Wilson Central Composite Face Centred (CCF, α: $\pm$ 1) design. The results were analysed with an analysis of variance (ANOVA) with 95% confidence and the cause-effect Pareto principle was used to determine their relative influence on the process. This corresponds to a 2^k factorial design, where k indicates the number of factors studied (in this case 3 operating variables) and 2^k represents the number of runs (in this case 8) for the simple factorial design. 8 axial experiments were performed to study non-linear effects and interactions according to the CCF design. In addition, four replicates at the

centre point (centre of the variation interval of each factor) were carried out in order to evaluate the experimental error.

The response variables studied were: the glycerol conversion (Xgly, %) and the carbon conversion to gas, liquid and solid products (CC gas, CC liq and CC sol, %), the composition of the gas (vol.%) and the liquid condensate (relative chromatographic area free of water and unreacted glycerol, %). The CC sol includes both the carbon deposited on the catalyst (coke) and the char. The used catalyst was characterised by elemental analysis to calculate the amount of carbon deposited on the catalyst surface. The CC coke and the amount of C deposited with respect to the amount of catalyst and organics (glycerol, acetic acid and methanol) reacted (mg C/g catalyst g organics reacted) were calculated from these analyses. CC char was therefore calculated by difference. Table 2 summarises the response variables and the analytical methods used for their calculation.

2.4 Data analysis

Firstly, the evolution over time was studied. For each experiment, the results are divided into three intervals. Each interval corresponds to the average value of the studied variables obtained during 40 minutes of experiment. All these values (three per experiment) have been compared using a one-way analysis of variance (one-way ANOVA) and Fisher´s least significant difference (LSD) test, both with 95% confidence. The results of the ANOVA analyses are provided as p-values. P-values lower than 0.05 indicate that at least two values are significantly different. The LSD test was used to compare pairs of data, i.e. either between two intervals of the same experiment or between two intervals of two different experiments. The results of the LSD tests are presented graphically in the form of LSD bars. To ensure significant

differences between any pairs of data, their LSD bars must not overlap.

Secondly, the effect of the operating variables has been studied considering the results corresponding to the first 40 minutes of reaction using a statistical analysis of variance (one-way ANOVA) test with 95% confidence. This avoids including the activity variation with time in the analysis. The ANOVA analysis helped to select the operating variables and interactions that significantly influence the response variables under consideration. In addition, the cause-effect Pareto principle was also used to calculate their relative importance.

In the simulations made for the theoretical study and in the fluidised bed experiments, the lower and upper limits of all the factors (temperature, glycerol concentration and liquid and N_2 flow rates in the theoretical study and temperature, glycerol concentration and $W/m_{glycerol}$ ratio in the experimental study) were normalised from -1 to 1 (codec factors). This codification permits all factors to vary within the same interval and helps to investigate their influence in comparable terms.

3. Results and discussion

3.1 Glycerol purification

The crude glycerol was neutralised with acetic acid. Different final pH values (5, 6 and 7) were used to evaluate the influence of the pH on the purity of the glycerol as well as on the facility and velocity of separation of the two liquid phases. Table 3 lists the chemical composition of the different glycerol solutions.

After this neutralisation, two phases appeared. The rest of the biodiesel and the free fatty acids constituted the upper phase. The bottom phase was made up of the excess of methanol used during the transesterification, acetic acid used during the neutralization, KOH used as catalyst in the transesterification step and glycerol obtained as a by-product. The fastest separation between phases and the glycerol with the highest purity was obtained using a final pH of 6. When a final pH of 7 was used, a complete separation of phases was not achieved, and a small layer was observed between the two phases. In addition, a complete removal of the FAMES of the crude glycerol was also achieved when a pH of 6 was used and consequently this final pH was selected. After that, this neutralised glycerol solution (pH=6) was subjected to a vacuum distillation where the methanol and acetic acid were partially removed from the solution. This refined glycerol (6*), obtained with a final pH=6 and subsequently subjected to vacuum distillation, was characterised and further used for the catalytic steam reforming experiments.

The chemical analysis of this refined glycerol is listed in Table 3. It shows an increase in glycerol concentration (up to 85 wt.%) and a decrease in the concentration of methanol and acetic acid, since they were separated from the solution. This strategy permits their further utilisation, thus improving the economy of the process. The ultimate analysis of the refined glycerol (in dry basis) is as follows: 36.33±0.65% C, 7.55±0.03% H and 56.11±0.63% O. The density, viscosity and LHV are 1.043±0.001 g/mL, 247.41±3.93 mPa·s and 16.96±0.03 MJ/kg, respectively. The purification step increases the viscosity and reduces the LHV of the glycerol solution in comparison to the values for crude glycerol due to the reduction of the methanol and FAMES content.

However, the LHV of this refined glycerol is still higher than that of reagent grade glycerol [15, 16].

3.2 Thermodynamic results

Table 4 shows the simulations performed and the results obtained in the theoretical study. The simulations predict a complete transformation of the glycerol, acetic acid and methanol present in the refined glycerol to H_2, CO_2, CO and CH_4 within the whole range of temperature and crude glycerol concentrations (S/C ratios) studied in this work. For each gas an empirical model that relates the operating variables (temperature, glycerol concentration, N_2 and liquid flow rates) to the volumetric composition of the gas was developed according to the ANOVA analysis and the relative influence of each factor in the model was calculated making use of the cause effect Pareto principle. The results of these analyses are summarised in Table 5.

The ANOVA analysis reveals that the temperature, the glycerol concentration, the liquid flow rate and the N_2 flow rate have a statistically significant influence on the equilibrium composition of the gas (p-values < 0.05). However, considering their relative influence, the gas composition is strongly affected by the temperature, the glycerol concentration and an interaction between these two variables. The relative influence of these variables in the process is higher than 75% for all the gases. This justifies the fact that the vast majority of works concerning steam reforming of glycerol only study the effect of the glycerol concentration (or steam to carbon ratio, S/C) and the temperature on the thermodynamics of the process [2]. The influence of the liquid and N_2 flow rates is related to variations in the partial pressures inside the reactor, which

affect the thermodynamic equilibrium. These small variations were also reported by Chen et al. [20] who studied the effect on the thermodynamics of the presence of an inert compound such as N_2.

Taking this information into account, two different models were developed: a full model and a simplified model. The former was used only for prediction purposes and includes all the significant effects and interactions of the four operating variables. The latter only includes the effect of the temperature, glycerol concentration and temperature-glycerol interactions. Table 5 displays the terms of the simplified models and the relative importance of all the variables according to the Pareto test. The effect of the N_2 and liquid flow rates and their interactions has been grouped together in the term "others". The lack of fit for all the simplified models is not significant in comparison to the pure error and their R^2 is higher than 0.98 in all cases. This indicates that they are able to predict up to 98% of the variations observed, confirming the little effect of the liquid and N_2 flow rates on the thermodynamic results of this work.

According to the analysis shown in Table 5, the temperature exerts the highest influence on the equilibrium composition. In addition, the quadratic effect for the temperature (T^2) is significant, which indicates that the evolution of the volumetric concentration of each gas is not linear with the temperature and the existence of maxima and minima. Additionally, the glycerol concentration and its interaction with the temperature are also significant. The effect of the temperature is related to the variation with temperature of the thermodynamic equilibrium constant of all the reactions involved in the process. The effect of the concentration of glycerol is related to the variations in the water content of the solutions (variations in the S/C ratio). The lower the concentration of

glycerol, the higher the excess of water and the S/C ratio. High S/C ratios help to shift the WGS and the methane reforming reactions towards the formation of H_2 [2]. These findings are in accordance with other works in the literature such as Hajjaji et al. [34], and Silva et al. [5]. These studies reported that the reforming temperature exerts a greater impact than the S/C ratio on the thermodynamic results.

The coefficients in the model for the temperature and the glycerol concentration show how an increase in temperature augments the concentration of H_2 and CO in the gas and decreases the amount of CO_2 and CH_4 in the gas (positive and negative values for the linear effect of the T in the model, respectively). In addition, an increase in the glycerol concentration decreases the concentration of H_2 and CO_2 in the gas, augmenting the proportion of CO and CH_4.

To fully study the effect of these two variables on the thermodynamics of the process, Fig. 1 displays the interaction plots between the temperature and glycerol concentration obtained from the statistical analyses. Specifically, the volumetric gas composition (vol.%) is plotted as a function of the temperature for the lowest and the highest (10 and 50 wt.%) glycerol concentrations employed in this work. The greatest increase for the H_2 content in the gas takes place between 400 and 600 ºC. A further increase up to 700 ºC has a negligible effect, indicating that a temperature between 600 and 650 ºC is optimum for H_2 production. These results can be explained taking into account the decomposition reactions for all the organics present in the refined glycerol solution: glycerol, acetic acid and methanol (Eq. 1, 2 and 3) as well as the water gas shift (WGS) equilibrium (Eq. 4).

$$C_3H_8O_3 \rightarrow 3CO + 4H_2 \quad \text{(Eq.1)}$$

$$CH_3COOH \rightarrow 2\ CO + 2\ H_2 \quad \text{(Eq.2)}$$

$$CH_3OH \rightarrow 2\ H_2 + CO \quad \text{(Eq.3)}$$

$$CO + H_2O \Leftrightarrow CO_2 + H_2 \quad \text{(Eq.4)}$$

The decomposition reactions of glycerol [2], acetic acid [35] and methanol [36] are highly endothermic and the water gas shift reaction is moderately exothermic [35], giving an overall endothermic process. Thus, an increase in temperature augments the equilibrium concentration of H_2 and CO in the gas. Conversely, an increase in temperature decreases the proportion of CO_2 and CH_4 in the gas, due to the endothermic nature of the reforming (Eqs. 5-6) and dry reforming (Eq.7) of methane as well as the exothermic character of the WGS reaction, respectively [2].

$$CH_4 + H_2O \Leftrightarrow CO + 3\ H_2 \quad \text{(Eq. 5)}$$

$$CH_4 + 2\ H_2O \Leftrightarrow CO_2 + 4\ H_2 \quad \text{(Eq. 6)}$$

$$CH_4 + CO_2 \Leftrightarrow 2\ CO + 2\ H_2 \quad \text{(Eq.7)}$$

The effect of the temperature is different depending on the glycerol concentration, due to the significant interaction between these two variables. The lower the concentration of glycerol in the feed, the higher the excess of water. This excess of water shifts the WGS reaction towards the production of H_2 and reduces the importance of the effect of the temperature. Fig. 1 shows how an increase in the glycerol concentration from 10 to

50 wt.% decreases the concentration of H_2 and CO_2 (at temperatures higher than 490 ºC) and increases the proportions of CO and CH_4 in the gas. An increase in the concentration of glycerol decreases the excess of water in the feed, which provokes a lesser shift of the WGS reaction towards the production of H_2 and CO_2. Furthermore, this lower excess also reduces the extent of the methane reforming reactions (Eqs.5-6), increasing the proportion of CH_4 in the gas [4-6, 20, 37].

A temperature between 600 and 650 ºC is optimum for H_2 production. Within this temperature range, the thermodynamic potential H_2 selectivity (H_2 produced /maximum stoichiometric H_2 that could be produced considering the complete reforming of all organics of the solution to H_2 and CO_2) for refined glycerol solutions having a glycerol concentration of 10, 30 and 50 wt.% (S/C = 13.80, 3.38 and 1.28 mol H_2O/mol C) varies as follows: 99, 87 and 77%, respectively. These results justify the fact that the vast majority of the works studying the reforming of glycerol used temperatures between 625 and 700 ºC and a high excess of water in the feed (high S/C ratios) to maximise the production of H_2.

3.3 Catalytic steam reforming results

The experimental conditions used in the experiments are shown in Table 6. In this table the runs are classified according to their temperature instead of the usual classical factorial order for a better understanding.

3.3.1 Global glycerol conversion and carbon distribution: CC gas, CC liq and CC sol.

A complete and steady global glycerol conversion (X gly) was achieved in all the

experiments, indicating that all the glycerol present in the refined glycerol solution was converted into gas, liquid and solid products. Fig. 2 shows the CC gas, CC liq, CC sol obtained for the experiments in three intervals of 40 min. From the statistical analyses, significant differences between the results obtained in the experiments were found for the CC gas, CC liq and CC sol (p-values < 0.001). Specifically, they vary as follows: 5-100%, 0-55% and 0-95%, respectively.

Regarding the temporal evolution of the carbon distribution, increases and drops in the CC gas, CC liq and CC sol are detected in some experiments. A significant increase in the CC gas along with a decrease in the CC sol is detected for experiments 9*, 16 and 17. This behaviour could be the consequence of the presence of KOH in the refined glycerol solution. The presence of KOH could hinder the evaporation of the organic compounds in the feed, causing low initial CC gas and high CC sol. Inorganic salts in a water solution can decrease the evaporation rate of the other organic compounds [38], increasing the formation of carbonaceous deposits [39]. However, as the reaction takes place and KOH accumulates inside the reactor, their presence might have a positive catalytic effect, helping the gasification of these carbon deposits and consequently increasing the CC gas and diminishing the CC sol [40, 41]. The accumulation of salts in the catalyst bed was also reported in the work of Fermoso et al. [16]. In addition, the effect of the presence of KOH during glycerol steam reforming was observed in a previous work about the catalytic steam reforming of a reagent grade glycerol solution with different amounts of KOH, CH_3OH and CH_3COOH [42].

Experiments 9*, 16 and 17 were conducted at the same temperature, 550 ºC. A higher initial CC gas together with a lower initial CC sol is obtained for run 16 due to the

higher $W/m_{glycerol}$ ratio employed. The same variation over time (around 20%) takes place for experiments 9* and 16, since the same temperature and glycerol concentration (identical accumulation of KOH) was used, while in run 17 the variation overtime is smaller due to the smaller concentration of glycerol. These results suggest that the plausible catalytic effect of KOH might be added to the intrinsic effect of the catalyst, and that the amount of KOH accumulated inside the reactor depends on the glycerol concentration.

Decreases in the CC gas and CC liq together with increases in the CC sol are observed for experiments 2, 6 and 8, probably due to a small deactivation of the catalyst. Comparing experiments 2, 6 and 21, conducted at 700 ºC and employing a $W/m_{glycerol}$ ratio of 3 g cat min/g glycerol, two evolutions with time are observed. A decrease in the CC gas takes places in runs 2 and 6 while a steady CC gas is observed for run 21. This suggests that the presence of KOH can partially compensate for the deactivation of the catalysts due to its catalytic activity in the gasification of carbon deposits. According to these results, a compromise between the excess of water and the amount of KOH in the bed is also necessary, and could explain the steady CC gas obtained in run 21 (30 wt.% glycerol). The amount of KOH could have been insufficient for run 2 despite the high excess of water (10 wt.% glycerol), while the decay observed for run 6 might have been the consequence of the lower amount of water for the gasification, in spite of the greater accumulation of KOH (50 wt.% glycerol).

Furthermore, an increase for the CC gas is only noticed in some experiments conducted at 550 ºC, which might suggest that its catalytic effect in the process depends on the temperature, and it might only take place at temperatures around 550 ºC. The catalytic

effect of KOH could not occur at temperatures lower than 550 ºC, while higher temperatures can result in a partial volatilisation of the solid, decreasing its catalytic activity. To corroborate this hypothesis, the thermal decomposition of KOH was experimentally studied at 550 and 700 ºC. Water solutions having 3.3, 1.0 and 0.36 wt.% of KOH were prepared and calcined in a muffle furnace at 550 and 700 ºC during 3 hours. The mass loss turned out to be independent of the concentration for both temperatures. A negligible solid mass loss was observed at 550 ºC, while a mass loss of 19±1 % with respect to the initial KOH took place at 700 ºC, confirming the partial volatilisation of the solid. This demonstrates the significant effect of the temperature on the catalytic activity of KOH. Additionally, the comparison between experiments 6 and 8 (conducted at 700 ºC and 50 wt% glycerol concentration) shows a lower variation for experiment 8 due to the higher $W/m_{glycerol}$ ratio employed. Therefore, it is believed that the catalytic effect of KOH in the process requires a temperature of around 550 ºC, a certain amount of KOH accumulated in the bed and an appropriate S/C ratio.

To gain a better insight into the carbon deposition, the carbon deposited on the used catalysts was determined and the solid carbon distribution into char and coke was calculated. Table 7 lists the CC coke, CC char and the amount of C deposited on the catalysts during the reforming experiments. The results indicate that the vast majority of the CC sol is due to the formation of char (more than 93% of the total solid C). The statistical analysis of the amount of carbon reveals that the highest deposition (mg C/ g catalyst g organic) takes place at 400 ºC (groups A to F). In these cases, the experimental drop in the CC gas was not observed due to the low initial CC gas obtained during the experiments. When a temperature between 550 and 700 ºC was employed in the experiments, the amount of carbon deposited reduced sharply. The

amount of C deposited for runs 2, 6 and 21, carried out at 700 ºC, varies from 0.63 to 2.82 mg C/g catalyst g organics reacted. In a previous work where this catalyst was used for the catalytic reforming of the aqueous fraction of bio-oil in a fluidised bed for 2 h [19], steady CC gas and gas composition were reported with an amount of C deposited on the catalyst of 10 mg C/ g catalyst g organic reacted, which is in the same range as that obtained in this work. This explains the low catalyst deactivation observed in this work and suggests that coking is the main cause responsible for the catalyst deactivation. Other catalyst deactivation mechanisms such as ageing and sintering are not likely to occur under the operating conditions tested, as previously reported when using this catalyst for the reforming of an aqueous fraction of bio-oil [19].

The specific effect of the operating conditions as well as their possible interactions on the process has been studied considering the results obtained during the first 40 minutes of reaction. The models created in terms of codec factors considering the ANOVA analysis and the relative importance of each variable in the model according to the Pareto analysis are presented in Table 8.

The CC gas and the CC sol are strongly affected by the temperature. An increase in the reforming temperature increases the CC gas and decreases the CC sol. In addition, the temperature has a significant quadratic effect, which indicates the existence of minima and maxima. These results indicate that the temperature exerts a positive effect on the catalytic steam reforming of glycerol due to the endothermic nature of the process. Furthermore, the vaporisation of the feed is not favoured at low temperatures, which increases the CC sol. In addition, the presence of KOH in the solutions also hinders the vaporisation of the organics, increasing the CC sol. This effect is strengthened at low

temperatures. Inorganic salts in a water solution decrease the evaporation rate of the other organic compounds [38], which might result in a higher formation of carbonaceous deposits [39]. These tendencies with the temperature were also observed in other works dealing with crude glycerol [6, 15, 18]. The CC liq is strongly influenced by the $W/m_{glycerol}$ ratio. An increase in the $W/m_{glycerol}$ ratio provokes a decrease in the CC liq due to the positive kinetic effect of the catalyst towards the formation of gases from the refined glycerol and other liquid intermediate compounds.

Significant interactions between variables also influence the CC gas, CC sol and CC liq, as can be appreciated from the models displayed in Table 8. Figs. 3 and 4 illustrate the effect of these interactions on the carbon distribution results. Fig. 3 plots the CC gas and CC sol as a function of the temperature employing $W/m_{glycerol}$ ratios of 3 and 17 g catalyst min/g glycerol. The effect of both variables does not depend on the refined glycerol concentration, since the interaction TWC (temperature, W/m_{gly} ratio and glycerol concentration) is not significant. Thus, as an example, this interaction is only shown for a 30 wt.% glycerol solution (S/C=3.38 mol H_2O/mol C). Conversely, the triple interaction is significant for the CC liq. Fig. 4 displays the effect on the CC liq of the reforming temperature employing $W/m_{glycerol}$ ratios of 3 and 17 g catalyst min/g glycerol for a 10 wt.% and a 50 wt.% glycerol solution.

An increase in temperature from 400 to 700 ºC provokes an increase in the CC gas and decreases the CC solid. At low temperature the steam reforming reaction and the vaporisation of the feed are not favoured, which causes the vast majority of the organics present in the solution to form carbon deposits (char). This evolution of CC gas with temperature as well as char formation at low temperatures was also reported in other

works working with crude glycerol. Dou et al. [15] reported a complete CC gas between 550 and 700 ºC feeding a crude glycerol solution (70-90 wt.% glycerol, 15 wt.% methanol and FAMES) using a S/C of 3 mol H_2O/mol C. It is believed that a lower temperature than that of this work was needed due to the absence of KOH in the crude glycerol. Valliyappan et al. [18] catalytically reformed a crude glycerol solution (60 wt.% glycerol, 31 wt.% CH_3OH, 1 wt.% KOH, 7.5 wt.% H_2O) at 800 ºC, reporting a CC gas of 90%. Slinn et. al [6] used a crude glycerol solution (33 wt.% glycerol, 23 wt.% CH_3OH, 3.8 wt.% ash, 40 wt.% FAMES and 3.2 wt.% H_2O), which corresponds to a S/C ratio of 1.35 mol H_2O/mol C in the reforming experiments. They reported an increase in the CC gas from 40 to 85% with increasing the temperature between 500 and 800 ºC. In the present work a CC gas higher than 95% was achieved at 650 ºC and beyond feeding a refined glycerol solution regardless of the S/C ratio. These results indicate that the two-step strategy developed in this work allows high gas production from crude glycerol using lower temperatures than those reported in other works, which is beneficial having regard to the energetic aspects of the process.

The $W/m_{glycerol}$ ratio only has a significant effect at low temperatures. Specifically, between 400 and 550 ºC, an increase in the $W/m_{glycerol}$ ratio from 3 to 17 g catalyst min/g glycerol increases the CC gas and decreases the CC sol. In these conditions, an increase in the amount of catalyst might modify the reaction pathways thanks to the excess of water in the feed. Conversely, at temperatures higher than 550 ºC, both the reforming reaction and the vaporisation of the organics are favoured and an increase in the $W/m_{glycerol}$ ratio from 3 to 17 g catalyst min/ g glycerol does not have a significant effect on these variables. These results indicate that the lowest amount of catalyst employed in this work is high enough to achieve high CC gas (>92%) at temperatures

higher than 650 ºC.

Fig. 4 illustrates how the CC liq decreases as the $W/m_{glycerol}$ ratio increases from 3 to 17 g catalyst min/g glycerol. An increase in the amount of catalyst inside the reactor shifts the reforming process, decreasing the proportion of intermediate liquids. This fact makes it possible that for the highest $W/m_{glycerol}$ ratio (17 g catalyst min/g glycerol), negligible CC liq (< 2 %) are obtained within the whole range of temperatures and concentrations studied in this work. However, employing a $W/m_{glycerol}$ ratio of 3 g catalyst min/g glycerol, the CC liq shifts from 0 to 8% and the temperature exerts two different effects depending on the concentration of glycerol.

On the one hand, for a low concentration of glycerol (10 wt.%) in the refined glycerol solution, an increase in temperature from 400 to 700ºC increases the CC liq. This increase in temperature reduces the formation of carbonaceous deposits, decreasing the CC sol. On the other hand, as the glycerol concentration in the solution increases (50 wt.% glycerol), when a $W/m_{glycerol}$ ratio of 3 g catalyst min/g glycerol is used, the CC liq shows an opposite trend with the temperature. High glycerol concentrations increase the mass of KOH accumulated inside the reactor. At high temperatures (550-700 ºC), the positive catalytic effect of potassium hydroxide on the process helps the gasification of the carbonaceous deposits, causing the CC sol to drop. However, the small amount of catalyst and the low temperature do not favour the complete conversion of the organics into gases, which increases the formation of intermediate liquid products. In addition, the high partial pressure of reactants can also intensify liquid formation at low temperature for the 50 wt.% refined glycerol solution.

3.3.2 Effect of the operating conditions on the volumetric composition of the gas

Fig. 5 illustrates the composition of the gas obtained for the different experiments divided into three intervals of 40 minutes. The gas phase is made up of a mixture of H_2 (65-95 vol.%), CO_2 (2-29 vol.%), CO (0-18 vol.%) and CH_4 (0-5 vol.%). The ANOVA analysis reveals significant differences between the experiments and time intervals (p-values < 0.05). As regards the evolution of the gas composition over time, statistically significant increases and decreases are detected for some experiments. However, these variations are very small, especially for the concentrations of H_2 and CO_2. The specific effects of the operating conditions as well as their possible interactions on the volumetric composition of the gas were studied considering the results obtained during the first 40 minutes of reaction. Table 9 shows the results of the statistical analyses performed.

3.3.2.1 H_2 and CO_2

The temperature is the most important operating variable for the relative amount of H_2 and CO_2 in the gas. In addition, the quadratic effect of the temperature is significant, indicating the existence of maxima and minima. While the concentration of glycerol exerts a strong influence on the relative percentage of H_2 in the gas, being as important as the temperature, it has a weak impact on the proportion of CO_2. Significant interactions between variables are also detected. The effect of the operating conditions on the relative amounts of H_2 and CO_2 in the gas is plotted in Fig. 6. Specifically, Figs. 6 a and c show the effect on the concentrations of H_2 and CO_2 of the temperature using a 10 wt.% glycerol solution and $W/m_{glycerol}$ ratios of 3 and 17 g catalyst min / g glycerol.

Figs. 6 b and d plot these effects for a 50 wt.% glycerol solution.

Using a refined glycerol solution having a 10 wt.% of glycerol, an increase in the temperature from 400 to 600 ºC diminishes the concentration of H_2 and increases the concentration of CO_2. These trends are the consequence of the progressive reduction of the CC sol with the temperature (95% at 400 ºC and 15% at 600 ºC). At low temperatures, a great amount of the C fed forms carbon deposits, lowering the amount of C in the gas and consequently increasing and decreasing the concentrations of H_2 and CO_2, respectively. As the temperature increases, both the proportion of C in the gas increases and the reforming process is more favoured, helping the production of H_2. At temperatures higher than 650 ºC a high CC gas (>95%) is achieved and the H_2 content of the gas reaches its thermodynamic value. This causes a small increase in the proportion of H_2 (up to its thermodynamic value) when the highest amount of catalyst is used. As a result a high (>98%) potential H_2 selectivity (H_2 produced/stoichiometric maximum H_2) is achieved under these conditions (10 wt.% glycerol, T>650 ºC and $W/m_{glycerol}$ = 17 g catalyst min/g glycerol). In addition, a drop in the concentration of CO_2 also takes place. This drop is also related to the thermodynamics of the process, since an increase in temperature decreases the thermodynamic CO_2 gas composition.

For a refined glycerol solution with a 50 wt.% of glycerol two trends are observed. For a $W/m_{glycerol}$ ratio of 3 g catalyst min /g glycerol, a decrease and an increase, respectively, in the proportions of H_2 and CO_2 in the gas are observed when the reforming temperature increases from 400 to 700 ºC. Conversely, for a $W/m_{glycerol}$ ratio of 17 g catalyst min /g glycerol, the compositions of H_2 and CO_2 are little affected by the reforming temperature. This circumstance results from the compensation of kinetic

and thermodynamic effects. For this 50 wt.% glycerol solution, an increase in the temperature from 400 to 700 ºC increases the thermodynamic H_2 concentration from 31 to 64 vol.% and decreases the thermodynamic CO_2 composition from 25 to 16 vol.%. At low temperatures, the low C content of the gas hampers reaching the thermodynamic equilibrium, which experimentally results in a gas with a high H_2 content. However, as the temperature increases, the thermodynamic H_2 and CO_2 composition increases and decreases, respectively, even though the amount of C in the gas increases. As a result, the potential H_2 selectivity decreases up to 75%, which is slightly lower than the thermodynamic maximum potential H_2 selectivity (80%) at this temperature (700 ºC) due to liquid and solid formation.

As regards the effect of the $W/m_{glycerol}$ ratio, two different trends can be appreciated depending on the temperature. On the one hand, between 400 and 600 ºC an increase in the amount of catalyst from 3 to 17 g catalyst min/g glycerol decreases the proportion of H_2 and increases the proportion of CO_2 in the gas. At these temperatures, a higher amount of catalyst not only favours the gasification of the carbon deposits, leading to a gas with higher CO_2 and lower H_2 contents, but also helps achieve a further extension of the reforming reactions. Temperatures from 600 ºC and above allow reaching H_2 and CO_2 compositions close to the thermodynamic equilibrium using $W/m_{glycerol}$ ratios as low as 3 g catalyst min/ g glycerol.

The effect of the concentration of glycerol can be gathered by comparing Figs. 6 a and b and 6 c and d. This comparison reveals that an increase in the amount of glycerol in the solution from 10 wt.% to 50 wt.% decreases the proportion of H_2 in the gas within the whole range of temperatures studied. The proportion of CO_2 is higher at 400 ºC using a

glycerol concentration of 50 wt.%, while at 700 ºC it is higher using 10 wt.% of glycerol. At temperatures lower than 500 ºC, an increase in the concentration of glycerol in the feed augments the amount of KOH accumulated in the bed, leading to higher gasification of the carbonaceous deposits. An increase in the concentration of refined glycerol reduces the S/C ratio, which reduces the extent of the WGS reaction [2].

Different H_2 productions were reported in other works dealing with crude glycerol. Specifically, Dou et al. [15] achieved the highest H_2 production (CC gas= 100%; 67 vol.%) at 700 ºC. Valliyappan et al. [18] and Slinn et. al [6] needed to use a temperature of 800 (CC gas = 85%, 60 vol.% H_2) and 900 ºC (CC gas = 91%, 59 vol.% H_2), respectively, for maximising H_2 production. The absence of KOH in the work of Dou et al. [15] is responsible for the higher H_2 yield, while the elimination of the FAME content of crude glycerol in this novel two steps process accounts for the higher H_2 production of this work in comparison to that reported by Valliyappan et al. [18] or Slinn et. al. [6]

3.3.2.2 CO and CH_4

The operating variable with the greatest influence on the proportion of both CO and CH_4 in the gas is the glycerol concentration, followed by the temperature, which also has a very strong effect. The effect of the operating conditions on the relative amount of CO in the gas is represented in Figs. 7 a and b. Fig. 7 a shows the effect on the CO concentration of the temperature using a refined glycerol solution having 10 wt.% of glycerol and $W/m_{glycerol}$ ratios of 3 and 17 g catalyst min / g glycerol. Fig. 7 b plots these

effects for a refined glycerol solution with a 50 wt.% of glycerol.

The effect of the temperature is at its greatest when a refined glycerol solution with a 50 wt.% of glycerol is employed. This is a thermodynamic consequence. When solutions of 10 wt.% and 50 wt.% are used, an increase in temperature from 400 to 700 ºC varies the thermodynamic relative amount of CO in the gas from 0.36 to 2.96 vol.% and from 0.93 to 19.38 vol.%, respectively. This accounts for the higher variation with temperature observed for the 50 wt.% glycerol solution than that for the 10 wt.%. Higher S/C ratios help shift the water gas shift reaction towards H_2 production, which helps to make the effect of the temperature less important.

Furthermore, when a refined glycerol solution with a 50 wt.% of glycerol is used, an increase in the temperature from 400 to 550 ºC decreases the relative amount of CO in the gas for a $W/m_{glycerol}$ ratio of 3 g catalyst min/ g glycerol. An increase in temperature increases the kinetic of the WGS reaction. This decrease in CO does not take place employing a higher $W/m_{glycerol}$ ratio, since this higher amount of catalyst is able to shift the WGS even at low temperatures. A further increase in the temperature from 550 to 700 ºC augments the proportion of CO in the gas because of the thermodynamics of the process.

The $W/m_{glycerol}$ ratio is only significant at temperatures lower than 500 ºC, where an increase in the $W/m_{glycerol}$ ratio from 3 to 17 g catalyst min/g glycerol shifts the WGS reaction. At these temperatures, the WGS is not kinetically favoured, and therefore an increase in the amount of catalyst shifts this reaction. However, at higher temperatures,

an increase in the ratio $W/m_{glycerol}$, is not statistically significant. At these temperatures, the lowest amount of catalyst employed (3 g catalyst min/ g glycerol) is high enough to reach the thermodynamic CO composition. The effect of the glycerol concentration can be seen comparing Fig. 7 a with 7 b. An increase in the concentration of glycerol from 10 to 50 wt.% provides a gas with a higher concentration of CO due to the reduction of the S/C ratio.

Figs. 7 c, d and e display the effects of the operating variables on the relative amount of CH_4 in the gas. For this gas, the third order interaction Temperature-Concentration-W/m_{gly} (TCW) is not statistically significant; therefore, the effect of the variables can be explained in groups of second order interactions. Fig. 7 c plots the effect of the $W/m_{glycerol}$ ratio. Two tendencies are appreciated depending on the reaction temperature. For temperatures between 400 and 550 ºC, an increase in the $W/m_{glycerol}$ ratio from 3 to 17 g catalyst min/g glycerol increases the relative amount of CH_4 in the gas. At these temperatures the formation of carbonaceous deposits is favoured, and an increase in the amount of catalyst increases the amount of C in the gas. The formation of CH_4 is favoured within this range of temperatures, where the thermodynamics predicts a gas with a high CH_4 content (around 15 vol.%). Conversely, between 550 to 700 ºC, where the formation of carbonaceous deposits is less favoured, the same increment in the $W/m_{glycerol}$ ratio exerts a positive effect on methane reforming and the concentration of CH_4 descends to its thermodynamic value (1 vol.%).

Fig. 7 d illustrates the effect of the $W/m_{glycerol}$ ratio for glycerol concentrations of 10 and 50 wt.% at 550 ºC. At this temperature, an increase in the $W/m_{glycerol}$ ratio from 3 to 17 g catalyst min/g glycerol has two different consequences depending on the

concentration of the refined glycerol solution. For a refined glycerol solution with a 10 wt.% of glycerol, an increase in the amount of catalyst does not have a statistically significant effect, and a $W/m_{glycerol}$ ratio of only 3 g catalyst min/ g glycerol is high enough for CH_4 to reach the thermodynamic composition. The high value of the S/C ratio (13.8 mol H_2O/mol C) prevents methane formation. On the other hand, when a refined glycerol solution having a 50 wt.% of glycerol (S/C=1.28 mol H_2O/mol C) is used, the thermodynamic proportion of CH_4 in the gas increases dramatically. In this case higher $W/m_{glycerol}$ ratios are needed to achieve thermodynamic gas composition. This means that an increase in the $W/m_{glycerol}$ ratio, which increases the kinetic of the process, also increases the amount of CH_4 in the gas up to its thermodynamic value (4 vol.%).

Fig. 7 e shows the effect of the temperature and the glycerol concentration when a $W/m_{glycerol}$ ratio of 10 g catalyst min/g glycerol is used. Under these conditions, the effect of the temperature is not significant when a refined glycerol solution with a 10 wt.% glycerol is used. Conversely, when a solution having a 50 wt.% glycerol is used the effect of the reaction temperature becomes more significant. As the temperature increases from 400 to 550 ºC, an increment in the relative amount of CH_4 in the gas can be observed. In these conditions, the amount of C in the gas increases and the thermodynamic proportion of CH_4 is high due to the reduction of the S/C ratio. Therefore, the higher the temperature, the higher the proportion of CH_4, since the amount of C in the gas increases sharply. However, a further increase of temperature from 550 to 700 ºC diminishes the proportion of CH_4 due to the steam reforming reactions of this gas.

3.3.3 Liquid composition

The liquid phase is made up of a mixture of aldehydes (acetaldehyde and propanal), alcohols (methanol, ethanol, propanol and 1,2-propanediol), phenols (phenol and alkyl phenols), carboxylic acids (acetic acid and propionic acid), ketones (acetone, butanone and hydroxyacetone) and a small proportion of cyclic compounds (12-crown-4 and 15-crown-5). The composition of the liquid phase during steam reforming of a glycerol solution obtained from biodiesel production has never reported before. However, the presence of these compounds in the condensates is consistent with the pathway proposed by Lin et al. [2] during the reforming of reagent grade glycerol. In addition, it is worth mentioning that small amounts of acetic acid and methanol are present in the refined glycerol solution, which also explains their presence in the liquid phase.

Fig. 8 summarises the relative amount of each one of the different families of liquid compounds for the different experiments represented in 3 intervals of 40 minutes. The results from the statistical analysis (ANOVA) revealed significant differences in the concentrations of aldehydes, alcohols, phenols, carboxylic acids, ketones (p-values < 0.05). The results of the Fisher´s LSD test are also plotted in Fig. 8. The relative concentration for these compounds, expressed as relative chromatographic area, varies as follows. Aldehydes: 0-25 %, alcohols: 0-71%, phenols: 0-100%, carboxylic acids: 0-67% and ketones: 0-95%. Two trends can be appreciated analysing the evolution over time of these compounds. Aldehydes, ketones and phenols remain relatively steady, while high variations over time can be seen for alcohols and carboxylic acids. A small increase in the concentration of aldehydes is noticed for experiments 2 and 15. This increase takes place along with a decrease for ketones in experiment 15. The relative proportion of phenols decreases for experiments 4, 9 and 17 and increases for

experiment 14. Only drops are detected for the proportion of alcohols (experiments 2, 7, 13 and 20), while drops (experiments 2, 7, 14 and 21) and increases (experiments 4, 8, 13 and 20) take place for the proportion of carboxylic acids.

The specific effects of the operating conditions as well as their possible interactions on the liquid composition were studied considering the results obtained during the first 40 minutes of reaction. Fig. 8 shows that alcohols, carboxylic acids, phenols and ketones are the families of compounds with the highest variation during the first 40 minutes of experiment, and consequently they are the most influenced by the operating conditions. Thus, only the influence of the operating conditions on the proportion of these families has been studied. Table 10 shows the significant terms in the codec model and their relative influence in the process according to the cause-effect Pareto test and the ANOVA analysis.

The statistical analysis reveals that the temperature is the operating variable with the highest influence on the proportion of alcohols and carboxylic acids in the liquid. Specifically, the high importance of the T^2 in the codec models and its positive value for both compounds indicate a strong influence of the temperature as well as the existence of a minimum in the relative amounts of the compounds with temperature. The proportion of ketones is also strongly influenced by the temperature, but with the exact opposite trend. The effect of the glycerol concentration and the $W/m_{glycerol}$ ratio on the proportion of alcohols and carboxylic acids is weak. However, they exert a strong influence on the concentration of phenols and ketones. In addition, significant interactions between variables are also detected.

Fig. 9 summarises the effect of the operating variables and the most important interactions on the liquid product distribution according to the ANOVA analyses. Some plots predict relative areas slightly lower/higher than 0/100 % due to the experimental character of the models. The effect of the temperature on the relative proportion of alcohols and carboxylic acids is plotted in Figs. 9 a-d. For both compounds, a decrease and a posterior increase in their proportions in the liquid with temperature are observed, regardless of the glycerol concentration or the $W/m_{glycerol}$ ratio. A minimum with temperature occurs at temperatures around 550-580 ºC.

According to the pathway proposed by Lin et at. [2], alcohols and carboxylic acids are intermediate compounds in glycerol steam reforming. In addition, it is worth mentioning that the glycerol employed in this work contains methanol and acetic acid. The analysis of the liquid phase reveals that at a low temperature, alcohols and carboxylic acids basically consist of methanol and acetic acid, respectively. An increase in temperature from 400 to 550 ºC favours the reforming of both compounds, diminishing their proportion in the liquid phase. In addition, for a 10 wt.% glycerol solution, a sharper drop takes place as the $W/m_{glycerol}$ ratio augments from 3 to 17 g catalyst min/ g glycerol, indicating the positive catalytic effect of the catalyst in the reforming of these two impurities. This trend changes when the concentration of glycerol in the refined solution increases up to 50 wt.% for the highest $W/m_{glycerol}$ ratio. The higher the glycerol concentration, the higher is the amount of KOH in the feed. This KOH promotes a high initial char formation, diminishing the CC gas and CC liq. In these cases an increase in the $W/m_{glycerol}$ ratio favours the gasification of these

carbonaceous deposits, but causes the concentration of alcohols and carboxylic acids to increase.

At temperatures of 580 ºC and above, 1-2 propanediol is the most abundant alcohol, while carboxylic acids are made up of acetic and propionic acids. A high increase in the proportion of 1-2 propanediol is observed as the temperature increases up to 700 ºC. This compound can be formed by a dehydration followed by a hydrogenation of glycerol [2, 43, 44]. An increase in temperature favours the reforming of methanol, reduces char formation and increases glycerol reforming, augmenting the proportion of intermediate liquids. In addition, within this interval of temperature, an increase in the $W/m_{glycerol}$ ratio reduces the proportion of intermediate alcohols, as their transformations to gases increase.

These same tendencies are observed for the relative amount of carboxylic acids in the liquid: the proportions of acetic and propionic acids increase between 550 and 700 ºC. Considering the reforming route for glycerol, acetic acid is a final compound. This increase takes place together with an increase in gas production, indicating that the temperature shifts the process towards final liquid intermediates and gases [2, 43]. This result is consistent with the increase in the CC gas and the decrease in the proportion of ketones in the liquid observed in this work, as acetic acid can be produced from hydroxyacetone [2]. As happens for alcohols, an increase in the $W/m_{glycerol}$ ratio from 3 to 17 g catalyst min/g glycerol also decreases the proportion of acids in the liquid, as their transformation into gases becomes more favoured.

Figs. 9 e and f show the effect of the temperature on the relative amount of phenols as a function of the $W/m_{glycerol}$ ratio for glycerol solutions of 10 and 50 wt.%, respectively. Phenols are end products in glycerol steam reforming [2]. According to the experimental results of this work, their presence in the liquid phase is favoured at high temperatures and $W/m_{glycerol}$ ratios when employing low glycerol concentrations. The presence of phenols is not favoured when the glycerol concentration increases, as can be gathered from Fig. 9 f. For a 10 wt.% glycerol solution, an increase in temperature increases the proportion of phenols when a high $W/m_{glycerol}$ ratio is used. However, an initial increase followed by a drop is observed for the lowest $W/m_{glycerol}$ ratio. This decrease takes place along with an increase in the relative amount of acids. Phenols and acetic acids formation from hydroxyacetone are in competition [2].

The significant effects of the operating variables on the proportion of ketones are plotted in Figs. 9 g and h. The proportion of ketones is highly influenced by the temperature and glycerol concentration. Thus, in both figures the effect of the temperature is represented as a function of the glycerol concentration for $W/m_{glycerol}$ ratios of 3 and 17 g catalyst min/g glycerol, respectively. The temperature exerts two different effects depending on the glycerol concentration regardless of the $W/m_{glycerol}$ ratio employed. On the one hand, for a refined glycerol solution with a 10 wt.% of glycerol, the effect of the temperature is small and is only significant when a high $W/m_{glycerol}$ ratio is used. An increase in the amount of catalyst decreases the proportion of ketones in the liquid. On the other hand, when the glycerol concentration in the solution increases up to 50 wt.%, a high increase in the proportion of ketones is observed, reaching a maximum at temperatures of around 550 ºC. At this temperature hydroxyacetone is the main compound present in the liquid phase.

Hydroxyacetone can be obtained from the dehydration of glycerol during one of the first steps in glycerol reforming [2]. An increase in the glycerol concentration increases the amount of KOH and decreases the excess of water in the feed. KOH exerts a positive catalytic effect in dehydration reactions [45, 46]. In addition, the lower the excess of water, the greater is the shift of the dehydration reactions of glycerol. These two effects might lead to a high proportion of hydroxyacetone in the condensate. At temperatures higher than 550 ºC, the reforming reactions are favoured and this compound can be transformed into gases and/or other final liquid products such as alcohols, carboxylic acids and phenols [2]. This decay is consistent with the increase in the proportion of these latter compounds between 550 and 700 ºC, as previously described.

3.3.4 Theoretical prediction of optimal operating conditions within the range of study

Optimal conditions for hydrogen production were sought for this process making use of the experimental models developed. The predicted R^2 of all the models is higher than 0.90, allowing their use for prediction purposes within the range of study. The optimisation process comprises the minimisation of the temperature and the $W/m_{glycerol}$ ratio and the maximisation of the refined glycerol concentration. It also aims to maximise the CC gas, and the concentration of H_2 in the gas, minimising the drop over time for both variables.

To meet this objective, a solution that strikes a compromise between the optimum values for all the response variables was sought. To do so, a relative importance (from 1 to 5) was given to each one of the objectives in order to come up with the solution that

satisfies all the criteria. Table 11 lists the relative importance assigned to each variable as well as the criteria used in the whole optimisation. Taking these restrictions into account, the optimisation predicts a possible optimum for the process, with the highest value of desirability, at a temperature of 680 ºC, employing a $W/m_{glycerol}$ ratio of 3 g catalyst min/g glycerol and feeding a refined glycerol solution of 37 wt.%. These operating conditions provide a CC gas of 95%, a potential H_2 selectivity (H_2 produced/ maximum stoichiometric H_2) of 91% and a gas with the following volumetric composition: 67 vol.% H_2, 22 vol.% CO_2, 11 vol.% CO and 1 vol.% CH_4. For the scale-up of the process, the fluidisation velocity could be further studied and optimised to achieve an optimum reactor performance, as thoroughly discussed in the work of Dou et al. [33].

Experiment 21 was conducted using operating conditions (T = 700 ºC, $W/m_{glycerol}$ ratio = 3 g catalyst min/g glycerol and glycerol concentration = 30 wt.%) very close to the optimum and very similar results were experimentally obtained (CC gas = 98%, CC liq = 1 %, CC sol = 1%, 67 vol.% H_2, 23 vol.% CO_2, 10 vol.% CO and 1 vol.% CH_4). This proves validation for the theoretical prediction obtained making use of the experimental models developed with the ANOVA analysis in the optimisation process.

4. Conclusions

The valorisation process of a crude glycerol solution obtained from biodiesel production has been studied in this work by means of an initial purification step followed by catalytic steam reforming. The catalytic steam reforming of the refined glycerol has been evaluated both theoretically and experimentally in a fluidised bed reactor using a

Ni-based catalyst. The most important conclusions obtained from this work are summarised as follows.

1. The pH exerts a significant influence on the purification of glycerol when acetic acid is used. An optimum phase separation and glycerol purity (85 wt.% glycerol, 6 wt.% methanol, 4 wt.% acetic acid, 4 wt.% ashes and 1 wt.% water) were achieved using a final pH of 6 together with a vacuum distillation.

2. The thermodynamic study showed that the temperature and the glycerol concentration are the most important operating variables affecting the gas composition. An increase in temperature from 400 to 700 ºC increases the content of H_2 and CO in the gas, decreasing the proportions of CO_2 and CH_4. In addition, decreases in the concentrations of H_2 and CO together with increases in the proportions of CO_2 and CH_4 take place as the glycerol concentration in the refined glycerol solution increases from 10 to 50 wt.%.

3. In the experimental study, the operating variables with the highest influence on the CC gas and the CC solid are the temperature and the $W/m_{glycerol}$ ratio. An increase in the temperature from 400 to 700 ºC increases the CC gas, diminishing the CC solid. The $W/m_{glycerol}$ ratio exerts a significant effect at temperatures lower than 550 ºC. At these temperatures, an increase in the $W/m_{glycerol}$ ratio helps the gasification of the carbon deposits, increasing and decreasing the CC gas and CC solid, respectively.

4. Experimentally, the gas phase was composed of H_2, CO_2, CO and CH_4. The temperature exerts the highest influence on the gas composition. Thermodynamic gas composition is achieved at temperatures higher than 550 ºC. At high temperatures, the higher the $W/m_{glycerol}$ ratio, the greater is the shift of the reforming reactions towards the production of H_2. At temperatures higher than 650 ºC, a high H_2 production is achieved. Specifically, between 650 ºC and 700 ºC a potential H_2 selectivity (H_2

produced/stoichiometric maximum H_2) higher than 98% is achieved for a refined glycerol solution containing a 10 wt.% of glycerol and using 17 g catalyst min/g glycerol. Conversely, under this temperature range the H_2 potential selectivity decreases up to 75% as the concentration of glycerol in the solution increases up to 50 wt.%.

5. A mixture of aldehydes, alcohols, phenols, carboxylic acids, ketones and a small proportion of cyclic compounds constituted the liquid phase during the reforming of the refined glycerol. The temperature is the operating variable with the highest influence on the liquid product distribution. Methanol and acetic acid, the two main impurities of the refined glycerol solution, are the largest liquid compounds at low temperatures. An increase in temperature decreases their relative amounts, increasing the proportion of other intermediate liquid compounds in glycerol steam reforming such as phenols and ketones. Temperatures higher than 550 ºC decrease the proportion of these intermediate products and lead to the formation of the final products in glycerol steam reforming: acetic acid and 1,2-propanediol.

6. An optimum for this two-step valorisation method was found using a final pH of 6 in the neutralisation step with acetic acid, and a temperature of 680 ºC, a glycerol concentration of 37 wt.% in the refined glycerol solution and a $W/m_{glycerol}$ ratio of 3 g catalyst min/g glycerol in the steam reforming process. As a result, 95% of the carbon in the feed was converted to a gas with the following composition: 67 vol.% H_2, 22 vol.% CO_2, 11 vol.% CO and 1 vol.% CH_4, which corresponds to a potential H_2 selectivity (H_2 produced/ maximum stoichiometric H_2) of 91%.

Acknowledgements

The authors wish to express their gratitude to the Aragon Government (GPT group), European Social Fund and Spanish MINECO (projects ENE2010-18985 and ENE2013-41523-R) for providing financial support. In addition, Javier Remón Núñez would like to express his gratitude to the Spanish MINECO for the FPI grant awarded (BES- 2011-044856).

References

[1] R. Manosak, S. Limpattayanate, M. Hunsom, Sequential-refining of crude glycerol derived from waste used-oil methyl ester plant via a combined process of chemical and adsorption, Fuel Processing Technology, 92 (2011) 92-99.
[2] Y.-C. Lin, Catalytic valorization of glycerol to hydrogen and syngas, International Journal of Hydrogen Energy, 38 (2013) 2678-2700.
[3] A.B. Leoneti, V. Aragão-Leoneti, S.V.W.B. de Oliveira, Glycerol as a by-product of biodiesel production in Brazil: Alternatives for the use of unrefined glycerol, Renewable Energy, 45 (2012) 138-145.
[4] B. Dou, Y. Song, C. Wang, H. Chen, Y. Xu, Hydrogen production from catalytic steam reforming of biodiesel byproduct glycerol: Issues and challenges, Renewable and Sustainable Energy Reviews, 30 (2014) 950-960.
[5] J.M. Silva, M.A. Soria, L.M. Madeira, Challenges and strategies for optimization of glycerol steam reforming process, Renewable and Sustainable Energy Reviews, 42 (2015) 1187-1213.
[6] M. Slinn, K. Kendall, C. Mallon, J. Andrews, Steam reforming of biodiesel by-product to make renewable hydrogen, Bioresource Technology, 99 (2008) 5851-5858.
[7] X. Song, Z. Guo, Technologies for direct production of flexible H_2/CO synthesis gas, Energy Conversion and Management, 47 (2006) 560-569.
[8] B. Dou, B. Jiang, Y. Song, C. Zhang, C. Wang, H. Chen, B. Du, Y. Xu, Enhanced hydrogen production by sorption-enhanced steam reforming from glycerol with in-situ CO_2 removal in a fixed-bed reactor, Fuel, 166 (2016) 340-346.
[9] B. Dou, C. Wang, H. Chen, Y. Song, B. Xie, Continuous sorption-enhanced steam reforming of glycerol to high-purity hydrogen production, International Journal of Hydrogen Energy, 38 (2013) 11902-11909.
[10] R. Wess, F. Nores-Pondal, M. Laborde, P. Giunta, Single stage H_2 production, purification and heat supply by means of sorption-enhanced steam reforming of glycerol. A thermodynamic analysis, Chemical Engineering Science, 134 (2015) 86-95.
[11] B. Dou, Y. Song, C. Wang, H. Chen, M. Yang, Y. Xu, Hydrogen production by enhanced-sorption chemical looping steam reforming of glycerol in moving-bed reactors, Applied Energy, 130 (2014) 342-349.
[12] B. Jiang, B. Dou, Y. Song, C. Zhang, B. Du, H. Chen, C. Wang, Y. Xu, Hydrogen production from chemical looping steam reforming of glycerol by Ni-based oxygen carrier in a fixed-bed reactor, Chemical Engineering Journal, 280 (2015) 459-467.
[13] S. Authayanun, A. Arpornwichanop, W. Paengjuntuek, S. Assabumrungrat, Thermodynamic study of hydrogen production from crude glycerol autothermal reforming for fuel cell applications, International Journal of Hydrogen Energy, 35 (2010) 6617-6623.
[14] K.S. Avasthi, R.N. Reddy, S. Patel, Challenges in the Production of Hydrogen from Glycerol- a biodiesel byproduct via steam reforming process, Procedia Engineering, 51 (2013) 423-429.
[15] B. Dou, G.L. Rickett, V. Dupont, P.T. Williams, H. Chen, Y. Ding, M. Ghadiri, Steam reforming of crude glycerol with in situ CO_2 sorption, Bioresource Technology, 101 (2010) 2436-2442.
[16] J. Fermoso, L. He, D. Chen, Production of high purity hydrogen by sorption enhanced steam reforming of crude glycerol, International Journal of Hydrogen Energy, 37 (2012) 14047-14054.

[17] N. Hajjaji, I. Baccar, M.-N. Pons, Energy and exergy analysis as tools for optimization of hydrogen production by glycerol autothermal reforming, Renewable Energy, 71 (2014) 368-380.
[18] T. Valliyappan, D. Ferdous, N.N. Bakhshi, A.K. Dalai, Production of hydrogen and syngas via steam gasification of glycerol in a fixed-bed Reactor, Topics in Catalysis, 49 (2008) 59-67.
[19] J. Remón, J.A. Medrano, F. Bimbela, L. García, J. Arauzo, Ni/Al–Mg–O solids modified with Co or Cu for the catalytic steam reforming of bio-oil, Applied Catalysis B: Environmental, 132-133 (2013) 433-444.
[20] H. Chen, Y. Ding, N.T. Cong, B. Dou, V. Dupont, M. Ghadiri, P.T. Williams, A comparative study on hydrogen production from steam-glycerol reforming: thermodynamics and experimental, Renewable Energy, 36 (2011) 779-788.
[21] B. Dou, C. Wang, Y. Song, H. Chen, Y. Xu, Activity of Ni–Cu–Al based catalyst for renewable hydrogen production from steam reforming of glycerol, Energy Conversion and Management, 78 (2014) 253-259.
[22] C. Wang, B. Dou, H. Chen, Y. Song, Y. Xu, X. Du, T. Luo, C. Tan, Hydrogen production from steam reforming of glycerol by Ni–Mg–Al based catalysts in a fixed-bed reactor, Chemical Engineering Journal, 220 (2013) 133-142.
[23] C. Wang, B. Dou, H. Chen, Y. Song, Y. Xu, X. Du, L. Zhang, T. Luo, C. Tan, Renewable hydrogen production from steam reforming of glycerol by Ni–Cu–Al, Ni–Cu–Mg, Ni–Mg catalysts, International Journal of Hydrogen Energy, 38 (2013) 3562-3571.
[24] X.D. Wang, S.R. Li, H. Wang, B. Liu, X.B. Ma, Thermodynamic Analysis of Glycerin Steam Reforming, Energy & Fuels, 22 (2008) 4285-4291.
[25] S. Adhikari, S. Fernando, S. Gwaltney, S. Filipto, R. Markbricka, P. Steele, A. Haryanto, A thermodynamic analysis of hydrogen production by steam reforming of glycerol, International Journal of Hydrogen Energy, 32 (2007) 2875-2880.
[26] S. Authayanun, A. Arpornwichanop, Y. Patcharavorachot, W. Wiyaratn, S. Assabumrungrat, Hydrogen production from glycerol steam reforming for low- and high-temperature PEMFCs, International Journal of Hydrogen Energy, 36 (2011) 267-275.
[27] Y. Li, W. Wang, B. Chen, Y. Cao, Thermodynamic analysis of hydrogen production via glycerol steam reforming with CO_2 adsorption, International Journal of Hydrogen Energy, 35 (2010) 7768-7777.
[28] J. Remón, F. Broust, J. Valette, Y. Chhiti, I. Alava, A.R. Fernandez-Akarregi, J. Arauzo, L. Garcia, Production of a hydrogen-rich gas from fast pyrolysis bio-oils: Comparison between homogeneous and catalytic steam reforming routes, International Journal of Hydrogen Energy, 39 (2014) 171-182.
[29] J. Remón, F. Broust, G. Volle, L. García, J. Arauzo, Hydrogen production from pine and poplar bio-oils by catalytic steam reforming. Influence of the bio-oil composition on the process, International Journal of Hydrogen Energy, 40 (2015) 5593-5608.
[30] J.A. Medrano, M. Oliva, J. Ruiz, L. Garcia, J. Arauzo, Catalytic steam reforming of acetic acid in a fluidized bed reactor with oxygen addition, International Journal of Hydrogen Energy, 33 (2008) 4387-4396.
[31] J.A. Medrano, M. Oliva, J. Ruiz, L. Garcia, J. Arauzo, Hydrogen from aqueous fraction of biomass pyrolysis liquids by catalytic steam reforming in fluidized bed, Energy, 36 (2011) 2215-2224.
[32] D. Kunii, O. Levenspiel, Fluidization Engineering, Second ed. Butterworth-Heinemann, Oxford, 1992.

[33] B. Dou, Y. Song, A CFD approach on simulation of hydrogen production from steam reforming of glycerol in a fluidized bed reactor, International Journal of Hydrogen Energy, 35 (2010) 10271-10284.
[34] N. Hajjaji, A. Chahbani, Z. Khila, M.-N. Pons, A comprehensive energy–exergy-based assessment and parametric study of a hydrogen production process using steam glycerol reforming, Energy, 64 (2014) 473-483.
[35] X. Hu, G. Lu, Investigation of the steam reforming of a series of model compounds derived from bio-oil for hydrogen production, Applied Catalysis B: Environmental, 88 (2009) 376-385.
[36] A. Iulianelli, P. Ribeirinha, A. Mendes, A. Basile, Methanol steam reforming for hydrogen generation via conventional and membrane reactors: A review, Renewable and Sustainable Energy Reviews, 29 (2014) 355-368.
[37] K. Kamonsuangkasem, S. Therdthianwong, A. Therdthianwong, Hydrogen production from yellow glycerol via catalytic oxidative steam reforming, Fuel Processing Technology, 106 (2013) 695-703.
[38] A.A. Zardini, I. Riipinen, I.K. Koponen, M. Kulmala, M. Bilde, Evaporation of ternary inorganic/organic aqueous droplets: Sodium chloride, succinic acid and water, Journal of Aerosol Science, 41 (2010) 760-770.
[39] R.P.B. Ramachandran, G. van Rossum, W.P.M. van Swaaij, S.R.A. Kersten, Evaporation of biomass fast pyrolysis oil: Evaluation of char formation, Environmental Progress and Sustainable Energy, 28 (2009) 410-417.
[40] C. Font Palma, A.D. Martin, Inorganic constituents formed during small-scale gasification of poultry litter: A model based study, Fuel Processing Technology, 116 (2013) 300-307.
[41] P. Nanou, H.E. Gutiérrez Murillo, W.P.M. van Swaaij, G. van Rossum, S.R.A. Kersten, Intrinsic reactivity of biomass-derived char under steam gasification conditions-potential of wood ash as catalyst, Chemical Engineering Journal, 217 (2013) 289-299.
[42] J. Remón, V. Mercado, L. García, J. Arauzo, Effect of acetic acid, methanol and potassium hydroxide on the catalytic steam reforming of glycerol: Thermodynamic and experimental study, Fuel Processing Technology, 138 (2015) 325-336.
[43] A. Wawrzetz, B. Peng, A. Hrabar, A. Jentys, A.A. Lemonidou, J.A. Lercher, Towards understanding the bifunctional hydrodeoxygenation and aqueous phase reforming of glycerol, Journal of Catalysis, 269 (2010) 411-420.
[44] Z. Yuan, J. Wang, L. Wang, W. Xie, P. Chen, Z. Hou, X. Zheng, Biodiesel derived glycerol hydrogenolysis to 1,2-propanediol on Cu/MgO catalysts, Bioresource Technology, 101 (2010) 7099-7103.
[45] H. Atia, U. Armbruster, A. Martin, Influence of alkaline metal on performance of supported silicotungstic acid catalysts in glycerol dehydration towards acrolein, Applied Catalysis A: General, 393 (2011) 331-339.
[46] J. Haber, K. Pamin, L. Matachowski, B. Napruszewska, J. Połtowicz, Potassium and silver salts of tungstophosphoric acid as catalysts in dehydration of ethanol and hydration of ethylene, Journal of Catalysis, 207 (2002) 296-306.

TABLES

Table 1. Properties of the crude glycerol. Results are presented as mean ± standard deviation.

Composition	
Glycerol (wt.%)	63.17±2.26
MeOH (wt.%)	34.37±2.13
Ashes (wt.%)	2.06± 0.23
H_2O (wt.%)	1.63±0.02
Ultimate Analysis	
C (%)	40.48±0.29
H (%)	8.19±0.06
O (%)[a]	51.33±0.34
TOC (ppm)	404733±2850
Physical properties	
pH	13.1±0.3
Density (g/mL)	1.060±0.001
Viscosity (mPa s)	49.93±1.48
LHV (MJ/kg)	21.89±0.05

[a] Determined by difference

Table 2. Response variables. Definitions and analytical techniques used in their determination.

Product	Response variable	Analytical method
Gas	$\text{CC gas (\%)} = \frac{\text{C in the gas (g)}}{\text{C fed (g)}} 100$	Micro Gas Chromatograph (Micro GC). N_2 as internal standard
	$\text{Composition (vol. \%)} = \frac{\text{mol of each gas}}{\text{total mol of gas}} 100$	Online analyses
Liquid	$\text{CC liq (\%)} = \frac{\text{C in the liquid products (g)}}{\text{C fed (g)}} 100$	Total Organic Carbon (TOC).
	$\text{Composition (area \%)} = \frac{\text{area of each compound}}{\text{total area}} 100$	GC-MS (Gas Chromatography-Mass Spectrometry).
	$\text{X gly (\%)} = \frac{\text{glycerol fed (g)} - \text{glycerol in the liquid (g)}}{\text{glycerol fed (g)}} 100$	GC-FID (Gas Chromatography-Flame ionization detector)
		Offline analyses
Solid	$\text{CC sol (\%)} = 100 - \text{CC gas (\%)} - \text{CC liq}^{*}\text{ (\%)}$	
	$\text{CC coke (\%)} = \frac{\text{C on the catalyst (g)}}{\text{C fed (g)}} 100$	Elemental Analysis.
		Offline analysis
	$\text{CC char (\%)} = \text{CC sol (\%)} - \text{CC coke (\%)}$	
	$\text{C (mg /g cat. g org.)} = \frac{\text{C on the catalyst (g)} * 1000}{\text{g catalyst g organics reacted}}$	

CC liq = Carbon conversion to liquid products (unreacted glycerol free).

CC liq* = Carbon conversion to liquids including unreacted glycerol

Table 3. Chemical analysis of the neutralised glycerol using different pH and the refined glycerol. Results are presented as mean ± standard deviation.

final pH	5	6	7	6 *
Composition				
Glycerol (wt.%)	48.62±2.79	54.03±0.05	53.10±2.11	85.25±0.79
CH_3OH (wt.%)	27.05±2.43	24.28±0.12	30.49±1.64	6.03±0.17
CH_3COOH (wt.%)	19.08±5.45	18.85±0.19	12.57±0.20	3.94±0.86
Ashes (wt.%)	5.26± 0.22	2.89± 0.01	3.84± 0.26	4.56± 0.37
H_2O (wt.%)	n.a.	n.a.	n.a.	1.38±0.002

* After vacuum distillation.

n.a. Not analysed

Table 4. Thermodynamic gas composition results for the simulations. The gas composition is expressed as the 95% confidence interval for the mean obtained with the different thermodynamic packages.

	Operating conditions								Equilibrium composition			
Simulation	**T (ºC)**		**[Glycerol] (wt%)**		**Liquid flow rate (mL/min)**		**N_2 Flow rate (mLN/min)**		**H_2 (vol%)**	**CO_2 (vol%)**	**CO (vol%)**	**CH_4 (vol%)**
	Actual	codec	actual	codec	actual	codec	actual	codec				
1	400	-1	10	-1	0.5	-1	225	-1	64.729 – 64.732	30.487 – 30. 487	0.338 – 0.338	4.444 – 4.447
2	700	1	10	-1	0.5	-1	225	-1	69.233 – 69.237	27.734 – 27.734	3.030 – 3.030	0 – 0.002
3	400	-1	50	1	0.5	-1	225	-1	28.658 – 28.662	35.976 – 35.976	0.846 – 0.847	34.517 – 34.520
4	700	1	50	1	0.5	-1	225	-1	63.786 – 63.789	16.277 – 16.277	19.489 – 19.489	0.446 – 0.449
5	400	-1	10	-1	1	1	225	-1	63.915 – 63.919	30.627 – 30.627	0.327 – 0.327	5.127 – 5.130
6	700	1	10	-1	1	1	225	-1	69.229 – 69.233	27.725 – 27.725	3.044 – 3.044	0 – 0.002
7	400	-1	50	1	1	1	225	-1	27.318 – 27.321	36.238 – 36.238	0.787 – 0.788	35.654 – 65.657
8	700	1	50	1	1	1	225	-1	63.669 – 63.673	16.348 – 16.348	19.419 – 19.420	0.560 – 0.563
9	400	-1	10	-1	0.5	-1	1347	1	68.169 – 68.172	29.887 – 29.887	0.391- 0.391	1.550 – 1.553
10	700	1	10	-1	0.5	-1	1347	1	69.234 – 69.238	27.735 – 27.735	3.030-3.030	0 – 0.002
11	400	-1	50	1	0.5	-1	1347	1	36.876 – 36.880	34.334 – 34.334	1.252 – 1.253	27.535 – 27.538
12	700	1	50	1	0.5	-1	1347	1	64.148 – 64.152	16.093 – 16.093	19.655 – 19.656	0.100 – 0.103
13	400	-1	10	-1	1	1	1347	1	66.712 – 66.715	30.141 – 30.141	0.369 – 0.369	2.776 – 2.779
14	700	1	10	-1	1	1	1347	1	69.234 – 69.237	27.735 – 27.735	3.030 – 3.030	0 – 0.002
15	400	-1	50	1	1	1	1347	1	32.829 – 32.832	35.156 -35.156	1.035 – 1.035	30.978 – 30.981
16	700	1	50	1	1	1	1347	1	64.032 – 64.036	16.164 – 16.164	19.585 – 19.586	0.215 – 0.218
17	550	0	30	0	0.75	0	786	0	66.406 – 66.410	26.500 – 26.500	5.290 – 5.290	1.801 – 1.804
18	400	-1	30	0	0.75	0	786	0	46.142 – 46.145	33.238 – 33.238	0.702 – 0.702	19.915 – 19.918
19	700	1	30	0	0.75	0	786	0	66.997 – 67.001	22.563 – 22.563	10.410 – 10.411	0.026 – 0.029
20	550	0	10	-1	0.75	0	786	0	69.695 – 69.699	28.874 – 28.874	1.410 – 1.411	0.017 – 0.020
21	550	0	50	1	0.75	0	786	0	57.532 – 57.536	24.826 – 24.826	9.447 – 9.448	8.192 – 8.195
22	550	0	30	0	0.5	-1	786	0	66.927 – 66.930	26.324 – 26.324	5.411 – 5.412	1.335 – 1.338
23	550	0	30	0	1	1	786	0	66.059 – 66.062	26.625 – 26.625	5.198 – 5.199	2.115 – 2.118
24	550	0	30	0	0.75	0	225	-1	65.092 – 65.095	26.944 – 26.944	4.982 – 4.983	2.978 – 2.981
25	550	0	30	0	0.75	0	1347	1	67.082 – 67.086	26.263 – 26.263	5.459 – 5.460	1.193 – 1.196

Table 5. Relative influence of the studied variables and interactions on the thermodynamic composition of the gas according to the ANOVA analysis for the simplified model.

	R^2	Intercept	T	C	TC	T^2	C^2	T^2C	Others
H_2 (vol.%)	0.98	65.91	9.12 (23)	-6.08 (24)	7.28 (17)	-8.82 (8)	ns	-3.86 (3)	(25)
CO_2 (vol.%)	1	26.49	-5.43 (42)	-1.64 (13)	-4.16 (30)	1.13 (3)	ns	ns	(12)
CO (vol.%)	1	5.30	5.26 (37)	4.25 (30)	3.97 (26)	0.37 (2)	0.24 (1)	ns	(4)
CH_4 (vol.%)	0.98	2.19	-8.95 (27)	4.09 (21)	-7.09 (20)	7.28 (10)	3.17 (3)	ns	(19)

ns: Non significant with 95% confidence

Response variable = Intercept + Coefficient $T \cdot T$ + Coefficient $C \cdot C$ + Coefficient $TC \cdot TC$ + Coefficient $T^2 \cdot T^2$ + Coefficient $C^2 \cdot C^2$ + Coefficient $T^2C \cdot T^2C$

Numbers in brackets indicate the percentage Pareto influence of each factor on the response variable. Pareto values represent the percentage of the orthogonal estimated total value.

The term "others" includes the Pareto influence of the liquid and N_2 flow rates and interaction in the thermodynamics. The effects of these factors were not included in this simplified model.

Table 6. Experimental operating conditions (actual and codec values) used in the fluidised bed experiments.

Experiment	T (ºC)		$W/m_{glycerol}$ (g cat min/g glycerol)		Glycerol concentration (wt.%)	
	actual	codec	actual	codec	actual	codec
1	400	-1	3	-1	10	-1
20	400	-1	3	-1	30	0
5	400	-1	3	-1	50	1
13	400	-1	10	0	30	0
3	400	-1	17	1	10	-1
7	400	-1	17	1	50	1
15	550	0	3	-1	30	0
17	550	0	10	0	10	-1
9* (9,10,11,12)	550	0	10	0	30	0
18	550	0	10	0	50	1
16	550	0	17	1	30	0
2	700	1	3	-1	10	-1
21	700	1	3	-1	30	0
6	700	1	3	-1	50	1
14	700	1	10	0	30	0
4	700	1	17	1	10	-1
19	700	1	17	1	30	0
8	700	1	17	1	50	1

Table 7. Solid carbon distribution. Overall 2 hours carbon conversion to solid, char and coke and C deposited on the catalyst.

Run	CC solid (%)	CC char (%)	CC coke (%)	C (mg C/g cat. g org.)
1	85.94 ^{A}	85.36 ^{A}	0.58 $^{D E}$	384 ^{A}
20	87.48 ^{A}	86.86 ^{A}	0.62 ^{D}	101.31 ^{B}
5	59.83 ^{D}	59.13 ^{C}	0.69 ^{D}	47.59 ^{C}
13	88.10 ^{A}	87.65 ^{A}	0.45 $^{D E F}$	21.25 ^{D}
3	77.25 ^{B}	77.02 ^{B}	0.23 $^{F G H}$	5.61 ^{F}
7	67.04 ^{C}	60.55 ^{C}	6.48 ^{A}	20.20 ^{D}
15	29.38 ^{E}	28.85 ^{D}	0.52 $^{D E}$	7.77 ^{E}
17	26.22 $^{E F}$	26.05 $^{D E}$	0.17 $^{G H}$	2.12 $^{H I J}$
9*	25.06 ± 1.03 ^{F}	24.55 ± 0.97 ^{E}	0.51 ± 0.07 $^{D E}$	1.95 ± 0.31 ^{J}
18	21.89 ^{G}	20.13 ^{F}	1.77 ^{B}	3.92 ^{G}
16	11.68 $^{H I}$	10.74 $^{G H}$	0.94 ^{C}	1.82 $^{I J}$
2	6.35 ^{K}	6.26 ^{J}	0.09 ^{H}	2.82 ^{HI}
21	8.59 $^{I J K}$	8.53 $^{H I J}$	0.06 ^{H}	0.63 ^{K}
6	13.40 ^{H}	13.03 ^{G}	0.37 $^{E F G}$	2.48 $^{H I J}$
14	0 ^{L}	0 ^{K}	0.16 $^{G H}$	0.45 ^{K}
4	10.74 $^{H I J}$	10.20 $^{G H I}$	0.54 $^{D E}$	3.04 $^{G H}$
19	0 ^{L}	0 ^{K}	1.70 ^{B}	2.86 $^{H I}$
8	7.55 $^{J K}$	7.29 $^{I J}$	0.26 $^{F G H}$	0.28 ^{K}

Letters in each column represent statistically significant groups with 90% confidence.

Table 8. Relative influence of the operating conditions on the CC gas, CC sol and CC liq according to the ANOVA analysis for the first 40 min of reaction.

Response	R^2	Intercept	T	W	C	T^2	W^2	C^2	TW	TC	WC	TWC	T^2W	TW^2	TC^2	WC^2	W^2C
CC gas (%)	0.97	67.68	39.66 (70)	5.58 (8)	ns	-10.57 (12)	ns	ns	-6.69 (10)	ns	ns	ns	ns	ns	ns	ns	ns
CC sol (%)	0.98	32.87	-38.21 (64)	-4.44 (6)	-4.36 (6)	14.61 (11)	-7.75 (5)	ns	5.86 (7)	ns	ns	ns	ns	ns	ns	ns	ns
CC liq (%)	0.94	0.79	ns ns	-2.25 (31)	ns	ns	2.29 (22)	ns	ns	-1.13 (8)	ns	1.37 (10)	2.5 (12)	-2.66 (13)	1.98 (4)	-2.03 (0)	ns

ns: Non significant with 95% confidence

Response = Intercept + Coefficient T · T + Coefficient W · W + Coefficient C C + Coefficient T^2 · T^2 + Coefficient W^2 · W^2+ Coefficient C^2 · C^2 + Coefficient TW · T·W + + Coefficient TC· T·C + Coefficient WC· W·C + Coefficient TWC ·T·W·C + Coefficient T^2W · T^2·W + Coefficient TW^2 ·TW^2 + Coefficient TC^2 · TC^2 + Coefficient WC^2 · W·C^2+ Coefficient W^2C · W^2C

Numbers in brackets indicate the percentage Pareto influence of each factor in the response variable. Pareto values represent the percentage of the orthogonal estimated total value

Table 9. Relative influence of the operating conditions on the gas composition according to the ANOVA analysis for the first 40 min of reaction.

Response	R^2	Intercept	T	W	C	T^2	W^2	C^2	TW	TC	WC	TWC	T^2C	T^2W	TW^2	TC^2	WC^2
H_2 (vol.%)	0.99	69.98	-7.31 (25)	-1.01 (4)	-3.44 (24)	5.6 (13)	-0.93 (2)	-1.36 (4)	2.19 (8)	3.42 (11)	ns	-1.13 (4)	-3.8 (6)	ns	ns	ns	Ns
CO_2 (vol.%)	0.99	25.16	4.95 (23)	ns	-3.88 (2)	-7.88 (27)	ns	-1.17 (3)	-2.34 (10)	-3.1 (12)	ns	0.48 (2)	4.29 (7)	2.71 (12)	ns	-0.73 (2)	ns
CO (vol.%)	0.99	3.83	2.44 (9)	ns	6.15 (36)	3.38 (14)	ns	2.11 (13)	0,88 (6)	ns	-0.72 (4)	0.77 (4)	ns	-1.89 (11)	-1.15 (3)	ns	ns
CH_4 (vol.%)	0.95	1.07	ns	ns	1.37 (18)	-0.98 (13)	0.50 (1)	0.49 (7)	-0.59 (17)	-0.60 (13)	0.74 (17)	ns	-0.84 (8)	ns	ns	ns	0.32 (6)

ns: Non significant with 95% confidence

Response = Intercept + Coefficient T · T + Coefficient W · W + Coefficient C C + Coefficient T^2 · T^2 + Coefficient W^2 · W^2+ Coefficient C^2 · C^2 + Coefficient TW · T·W + + Coefficient TC· T·C + Coefficient WC· W·C + Coefficient TWC ·T·W·C + Coefficient T^2C · T^2·C + Coefficient T^2W · T^2·W + Coefficient TW^2 ·TW^2 + Coefficient TC^2 · TC^2 + Coefficient WC^2 · W·C^2+ Coefficient W^2C · W^2C

Numbers in brackets indicate the percentage Pareto influence of each factor in the response variable. Pareto values represent the percentage of the orthogonal estimated total value

Table 10. Relative influence of the operating conditions on the liquid composition according to the ANOVA analysis for the first 40 min of reaction.

	R^2	Intercept	T	W	C	T^2	W^2	C^2	TW	TC	WC	TWC	T^2C	T^2W	TW^2	TC^2	WC^2
Alcohols (Area %)	0.99	7.31	-32.16 (23)	ns	2.1 (3)	32.74 (24)	-5.43 (5)	-2.79 (3)	-8.88 (9)	4.92 (6)	4.53 (5)	2.55 (3)	ns	7.62 (1)	ns	24.17 (11)	-11.33 (6)
Acids (Area%)	1	1.56	19.74 (3)	ns	0.90 (5)	19.68 (25)	-6.57 (9)	2.78 (6)	-0.58 (0)	-1.60 (3)	2.39 (5)	-3.50 (7)	1.81 (1)	-7.20 (3)	-23.19 (24)	-2.43 (2)	-2.24 (7)
Phenols (Area%)	0.98	44.76	ns	ns	-41.21 (16)	ns	-17.05 (8)	-16.62 (4)	8.36 (9)	-9.37 (8)	-11.44 (10)	-10.50 (9)	30.76 (12)	13.92 (5)	27.55 (13)	-14.72 (6)	ns
Ketones (Area%)	0.93	32.62	ns	ns	34.19 (16)	-42.95 (22)	33.16 (24)	15.07 (6)	ns	6.67 (8)	ns	Ns	-27.08 (14)	ns	ns	ns	ns

ns: Non significant with 95% confidence

Response = Intercept + Coefficient T · T + Coefficient W · W + Coefficient C C + Coefficient T^2 · T^2 + Coefficient W^2 · W^2+ Coefficient C^2 · C^2 + Coefficient TW · T·W + + Coefficient TC· T·C + Coefficient WC· W·C + Coefficient TWC ·T·W·C + Coefficient T^2C · T^2·C + Coefficient T^2W · T^2·W + Coefficient TW^2 ·TW^2 + Coefficient TC^2 · TC^2 + Coefficient WC^2 · W·C^2+ Coefficient W^2C · W^2C

Numbers in brackets indicate the percentage Pareto influence of each factor in the response variable. Pareto values represent the percentage of the orthogonal estimated total value

Table 11. Theoretical optimisation: operating conditions and response variables.

Objectives, interval of variations, relative importance and optimum values.

Variables	Objective	Interval of variation	Relative importance (1-5)	Optimum value
Temperature (ºC)	Minimise	400-700	4	680
$W/m_{glycerol}$ (g cat min/g glycerol)	Minimise	3-17	3	3
[Glycerol] (wt.%)	Maximise	10-50	5	37
CC gas (%)	Maximise	0-100	5	95
CC liq (%)	Minimise	0-100	3	1
CC sol (%)	Minimise	0-100	5	1
X gly (%)	Maximise	0-100	3	100
H_2(vol.%)	Maximise	0-100	4	67
CO_2(vol.%)	None	0-100		22
CO(vol.%)	None	0-100		11
CH_4(vol.%)	Minimise	0-100	4	1
Var CC (%)*	Minimise	None	2	-0,63

**Var CC(%) = Time variation percentage for the carbon conversion to gas. Positive and negative values indicate decrease and an increase of the CC gas over time.*

$$Var\ CC = -11.97 - 2.94\ W/m_{glycerol} + 8.74\ T^2 + 12.26\ [Glycerol]^2 + 3.25\ T\ [Glycerol]^2\ (R^2 = 0.82)$$

FIGURES

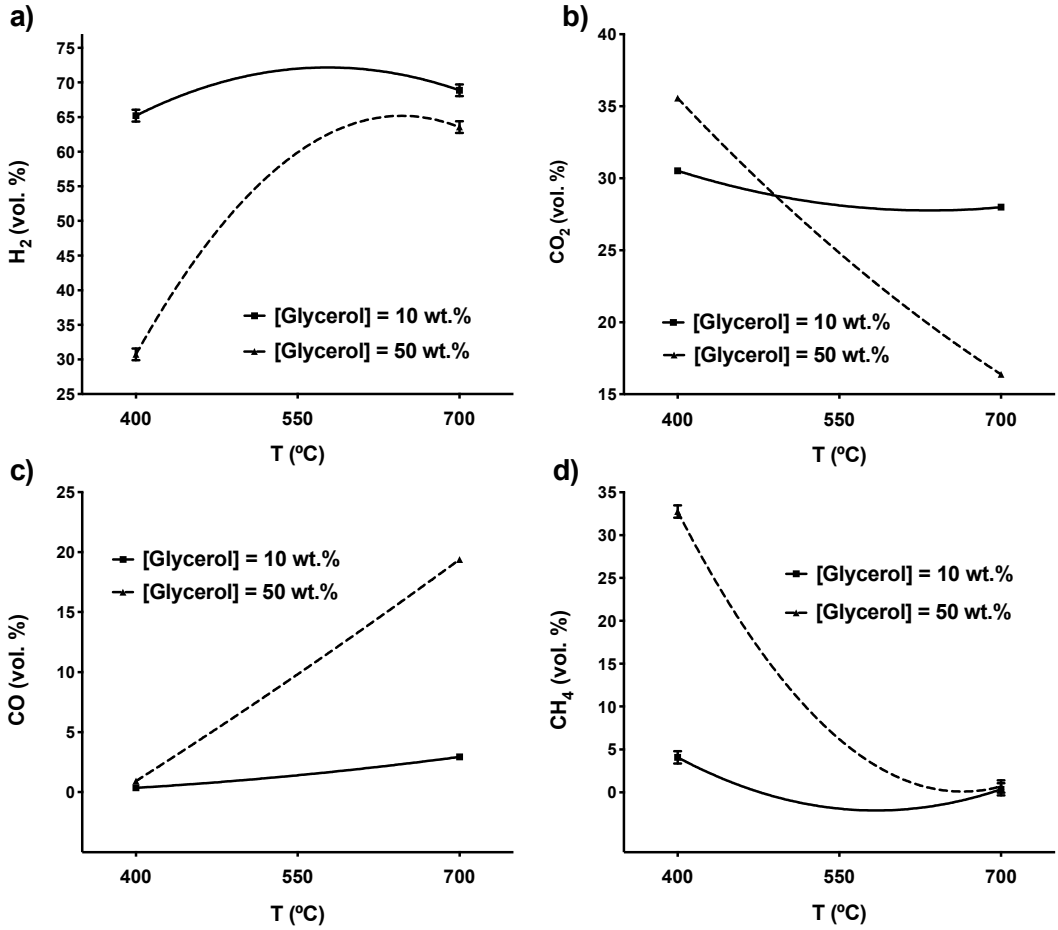

Fig.1. Evolution with temperature of the thermodynamic content (vol.%) of H_2 (a), CO_2 (b), CO (c) and CH_4 (d) in the gas as a function of the temperature for refined solutions having glycerol concentrations of 10 and 50 wt.% (S/C = 13.8 and 1.28 mol H_2O/mol C)

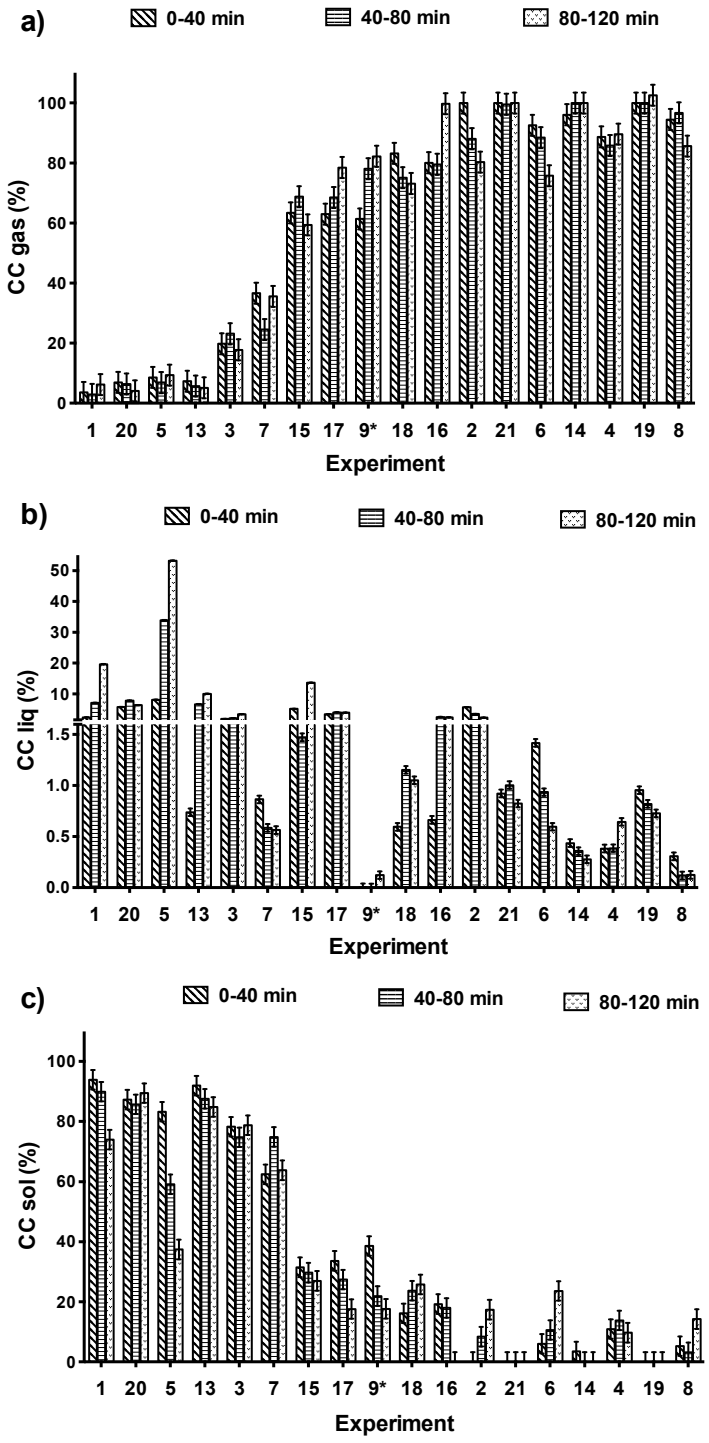

Fig.2. Carbon Conversion to gas (a), liquid (b) and solid (c) obtained during the reforming experiments. Results are presented as the overall values obtained each 40 minutes and expressed as mean ± 0.5 Fisher LSD intervals with 95% confidence.

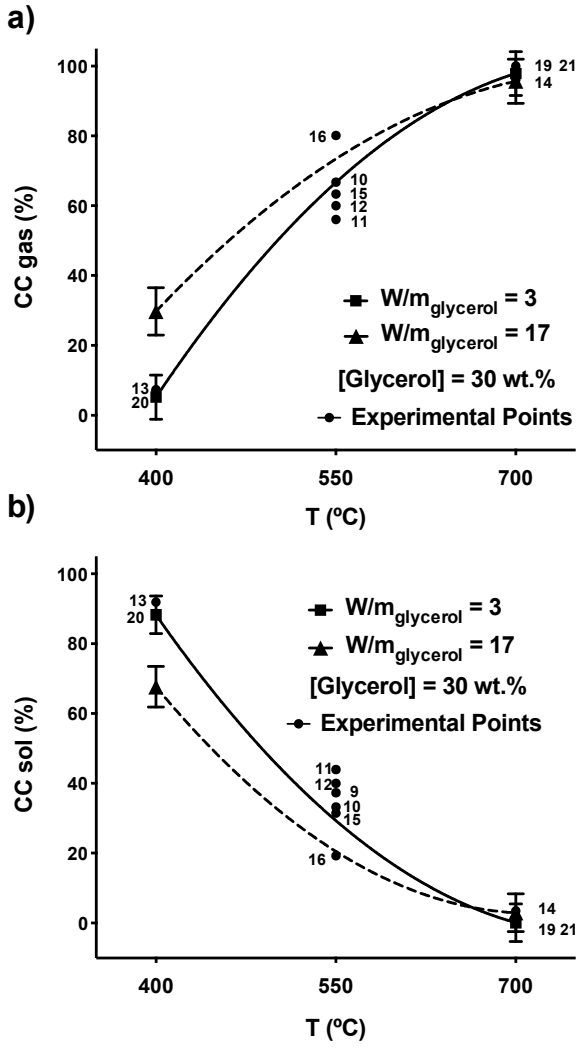

Fig.3. Interaction plots between temperature and $W/m_{glycerol}$ ratio for the initial CC gas (a) and CC solid (b) for a refined glycerol solution with a 30 wt.% of glycerol (S/C = 3.38 mol H_2O/mol C). Bars are LSD intervals with 95% confidence.

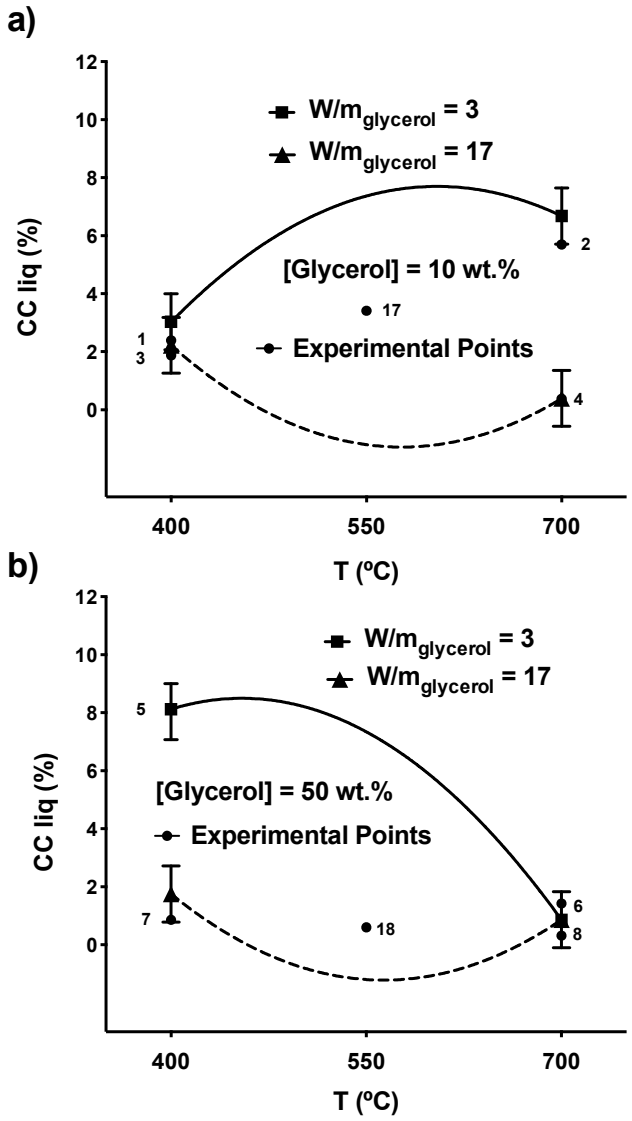

Fig.4. Interaction plots between temperature and $W/m_{glycerol}$ ratio for the initial CC liq using glycerol solutions with a glycerol concentration of (a) 10 wt.% (S/C = 13.8 mol H_2O/mol C) and (b) 50 wt.% (S/C = 1.28 mol H_2O/mol C. Bars are LSD intervals with 95% confidence.

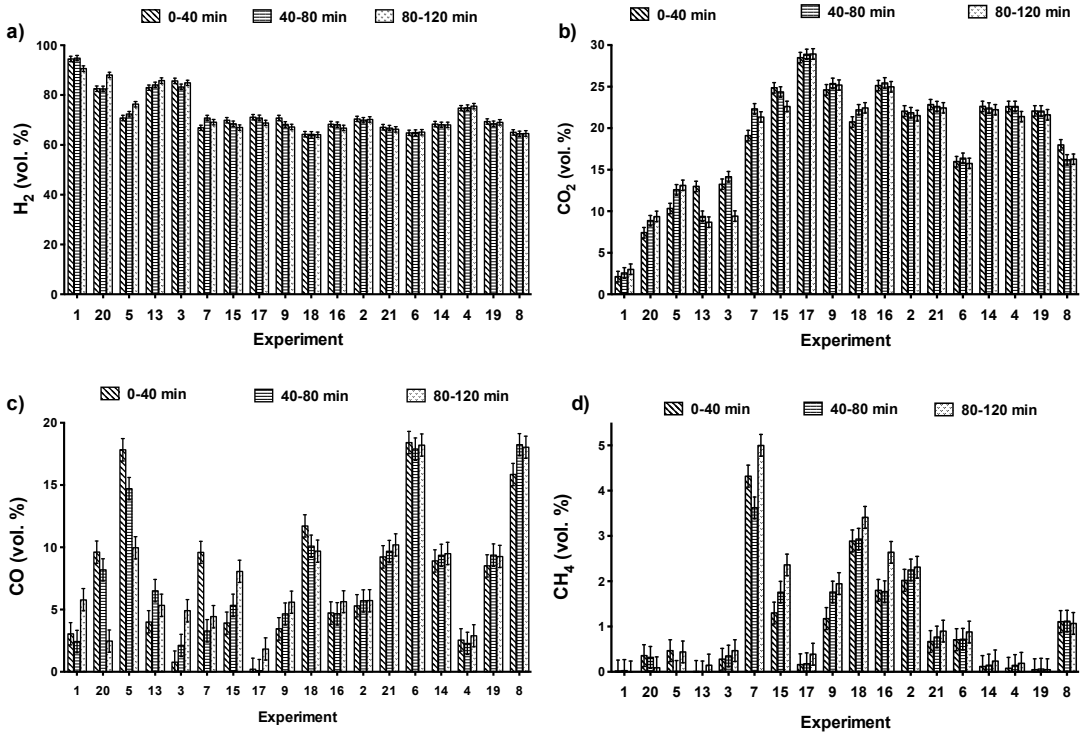

Fig.5. Relative amount (vol.%) of H_2 (a), CO_2 (b) CO (c) and CH_4 (d) in the gas obtained during the reforming experiments. Results are presented as the overall values obtained each 40 minutes and expressed as mean ± 0.5 Fisher LSD intervals with 95% confidence.

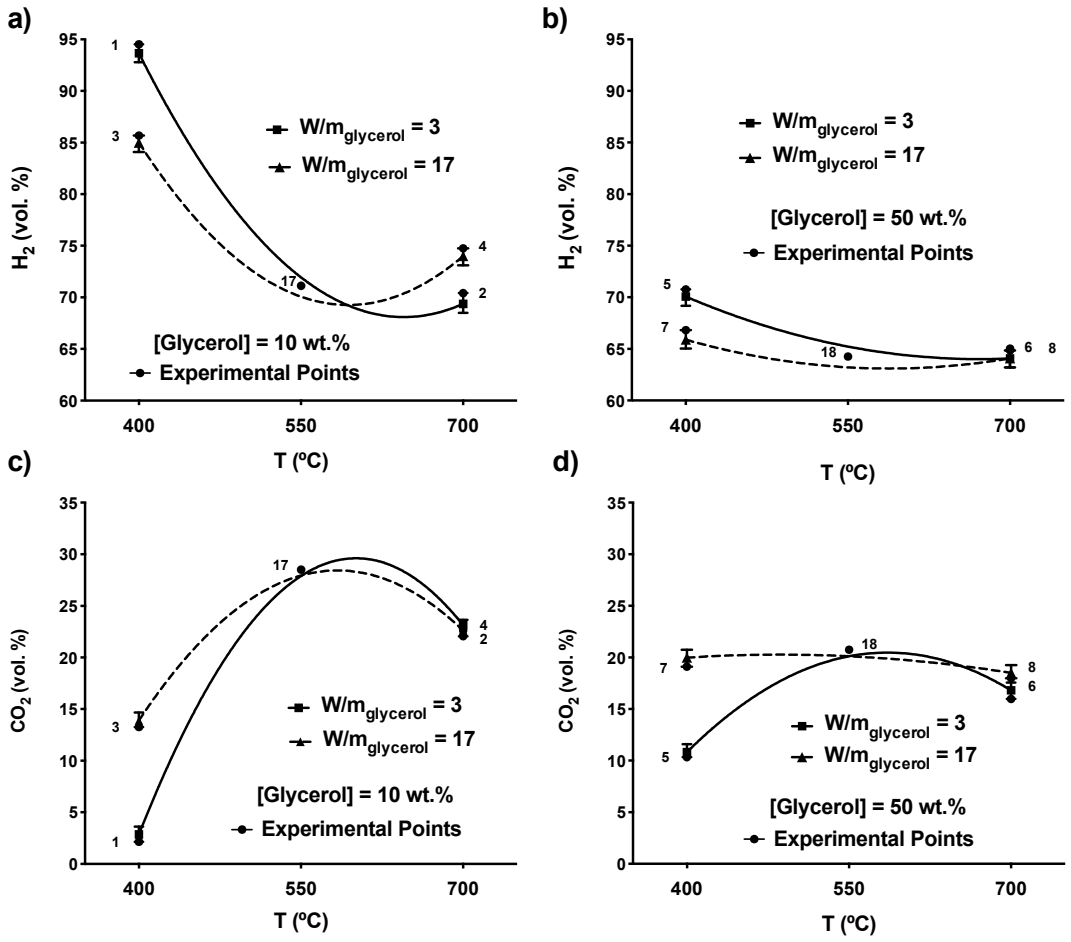

Fig.6. Interaction plots between temperature and $W/m_{glycerol}$ ratio for H_2 and CO_2 concentrations using refined glycerol solutions having (a and b) 10 wt.% of glycerol (S/C = 13.8 mol H_2O/mol C) and (c and d) 50 wt.% of glycerol (S/C = 1.28 mol H_2O/mol C). Bars are LSD intervals with 95% confidence.

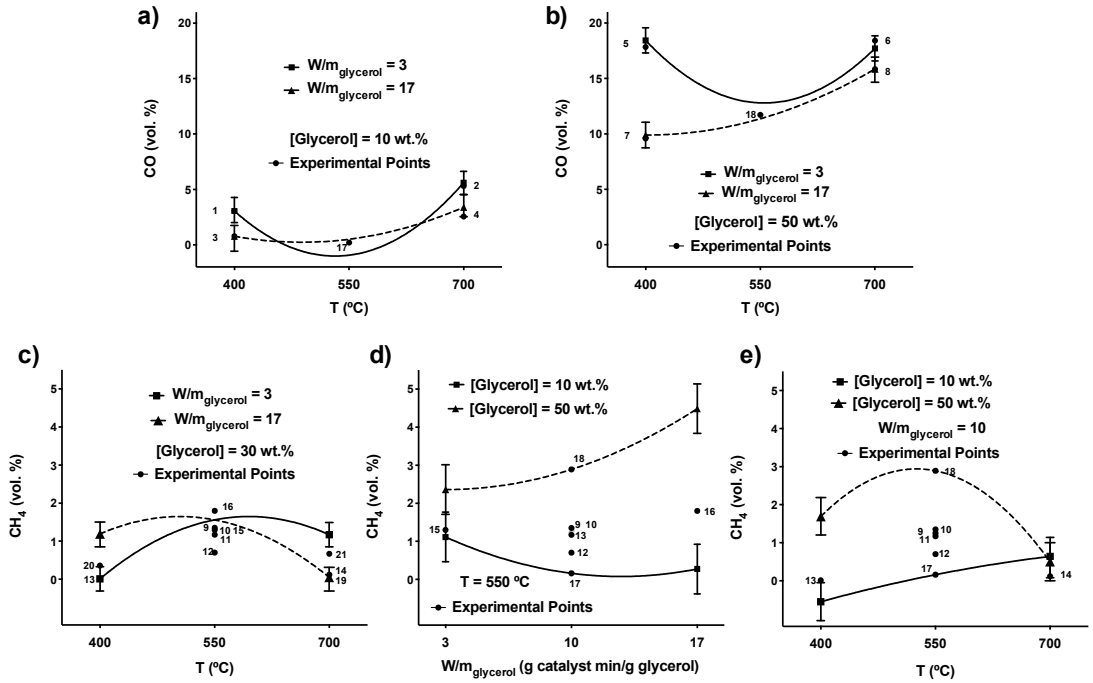

Fig.7. Interaction plots between temperature and $W/m_{glycerol}$ ratio for the proportion of CO concentrations using refined glycerol solutions with glycerol concentrations of (a) 10 wt.% (S/C = 13.8 mol H_2O/mol C) and (b) 50 wt.% (S/C = 1.28 mol H_2O/mol C). Interaction plots for the proportion of CH_4: (c) temperature-$W/m_{glycerol}$ ratio, (d) $W/m_{glycerol}$ ratio-glycerol concentration and (e) temperature-glycerol concentration. Bars are LSD intervals with 95% confidence.

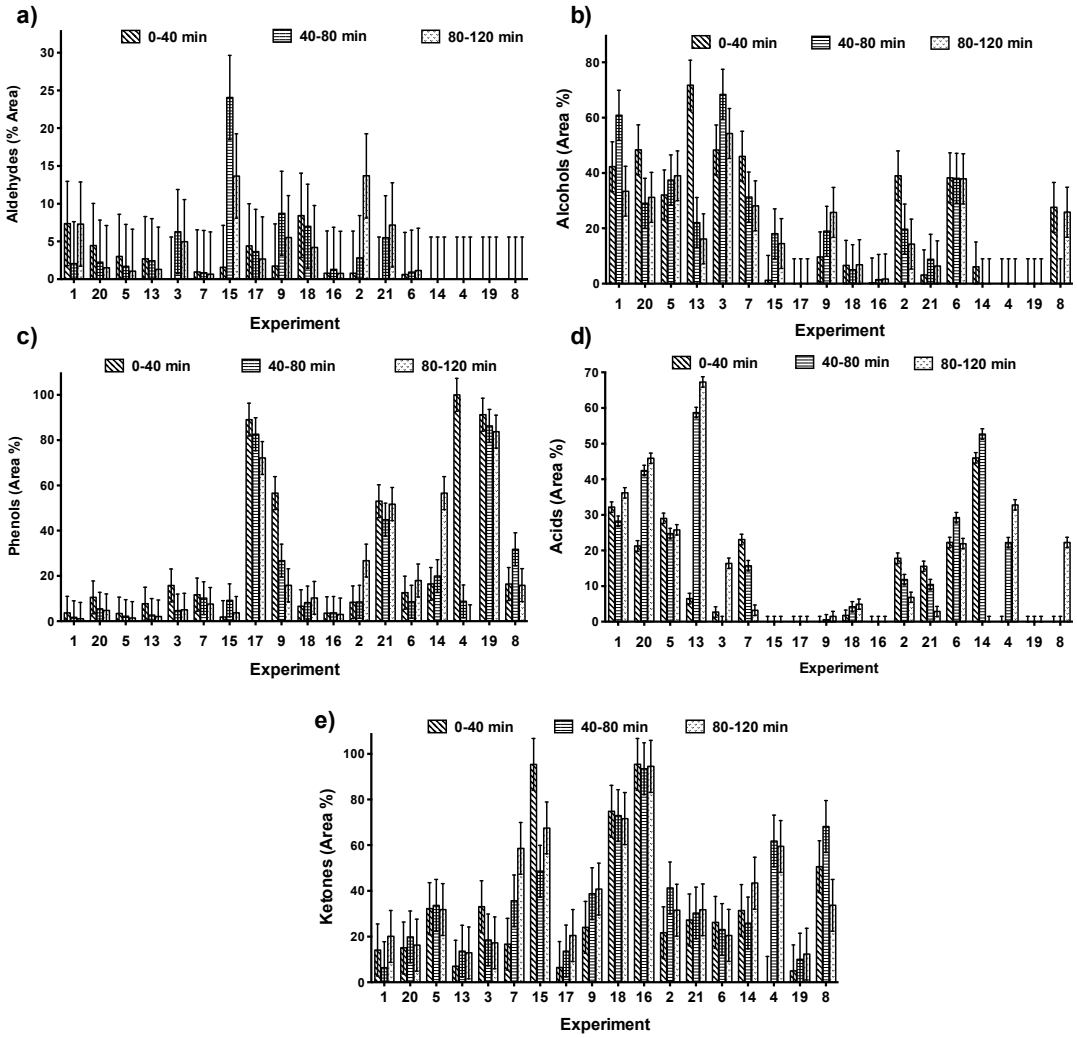

Fig.8. Relative amount (% chromatographic area) of aldehydes (a), alcohols (b), phenols (c), carboxylic acids (d), and ketones (e) obtained during the reforming experiments. Results are presented as the overall values obtained each 40 minutes and expressed as mean ± 0.5 Fisher LSD intervals with 95% confidence.

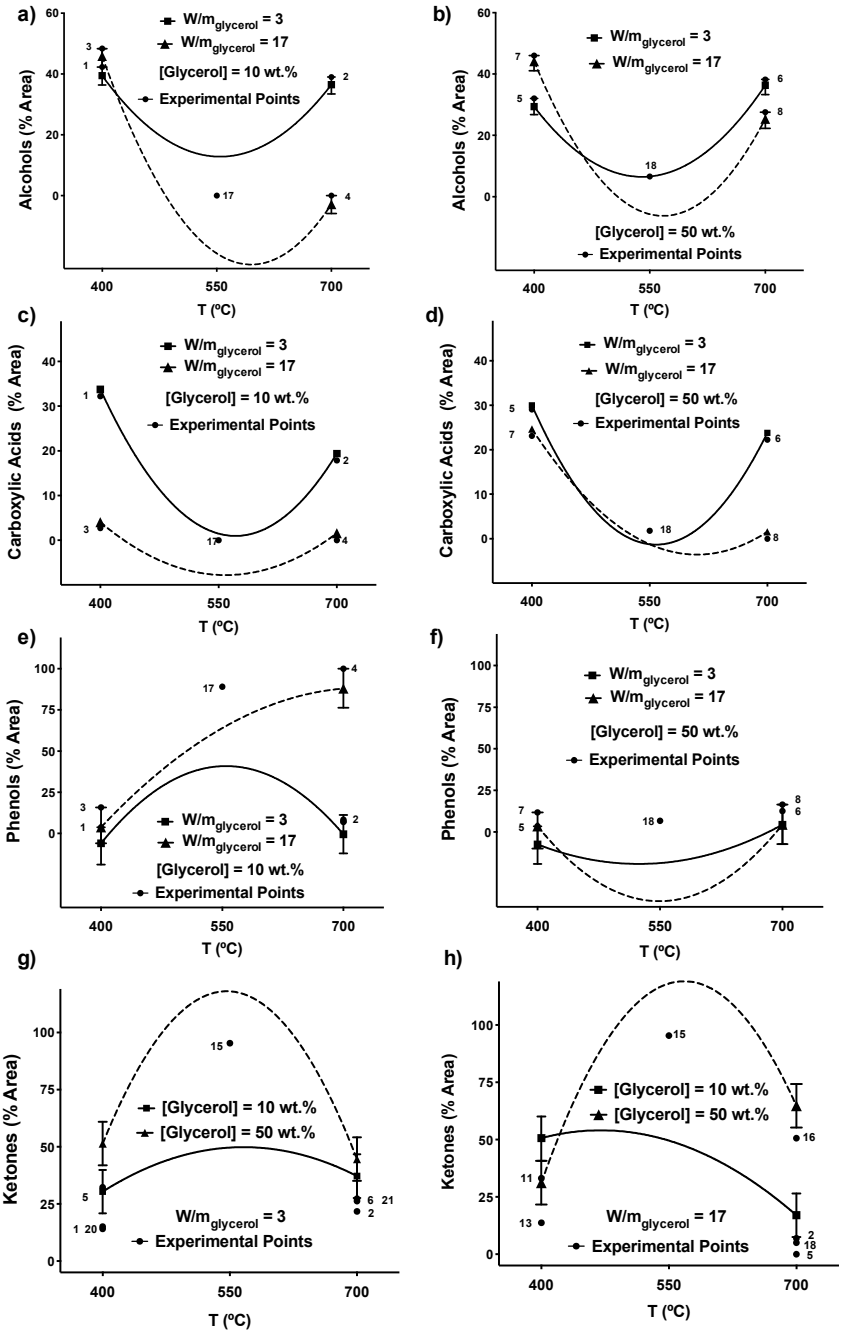

Fig.9. Interaction plots between temperature and $W/m_{glycerol}$ ratio using refined glycerol solutions having 10 and 50 wt.% of glycerol (S/C = 13.8 and 1.28 mol H_2O/mol C) for the relative amount of alcohols (a and b), carboxylic acids (c and d) and phenols (e and f). Interaction plots between the temperature and the glycerol concentration using $W/m_{glycerol}$ ratios of 3 and 17 g cat min/g org (g and h) for the relative amount of ketones. Bars are LSD intervals with 95% confidence.